EMPOWERING UNDERGROUND LABORATORIES NETWORK USAGE

**Activity Report of WP3.3** **12|2021**

# Scheme of GIG Experimental Mine 'Barbara' devoted to natural background radiation (NBR) characterization

**Author: Katarzyna Szkliniarz, Jan Kisiel**
**University of Silesia, Poland**

Interreg Baltic Sea Region
EUROPEAN UNION
EUROPEAN REGIONAL DEVELOPMENT FUND

## Contents

## Figures

## Tables

## 1. General information

Name of Underground Laboratory:

**GIG Experimental Mine 'Barbara'**

**(https://www.gig.eu/pl/kd-barbara)**

Localization (country/city):

**Poland/Mikołów**

Coordinates to the facility:
50° 10' 47.1" North
18° 55' 58.6" East

Altitude of the facility:
about 287 m


Name of the responsible scientist/measurer:
University of Silesia, Poland:
Jan Kisiel
Agata Walencik-Łata
Katarzyna Szkliniarz

National Centre for Nuclear Research, Poland:
Karol Jędrzejczak
Jacek Szabelski

Place where the data is stored (e.g. file in a drawer X, internal data cloud etc.):
pendrive, external memory,

## 2. Measurements of the NBR in Underground Laboratory

Description of the sites where the in-situ measurements were performed:

Tab. 1 Description of the sites where the in-situ measurements were performed.

| **Hall ID** | **Dimension of the cavern** [height x length x width] (m) | **Air volume exchange rate / Ventilation** [$m^3/s$] | **Depth below surface** [m w.e.] | **Environmental condition** (average temperature /average humidity) |
|---|---|---|---|---|
| blind chamber excavation | 2.65 x 30 x 3 | 30-40 | 122 | 12 °C / 70% |

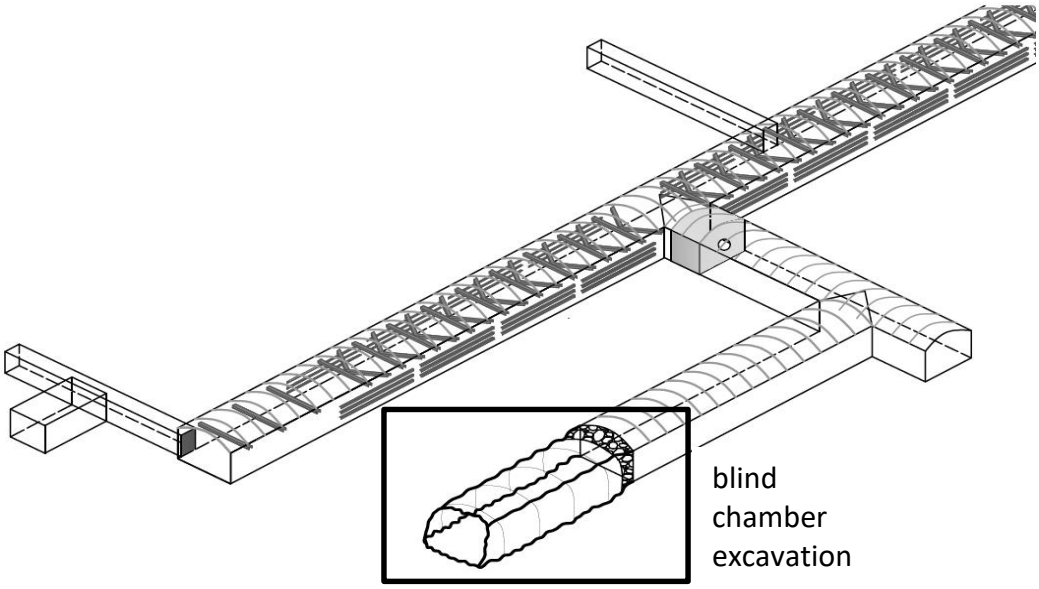


Fig. 1 Scheme of the workings where the in-situ measurements were performed.

### *a. In-situ gamma-ray measurement*

- Information about measurement

The in-situ measurement of the natural background radiation (NBR) was performed by using portable gamma-ray spectroscopy and HPGe (high-purity germanium) detector. For spectra registration and analysis, the multichannel analyzer and special software packages were applied. Energy calibration (covering the range of 14 – 2506 keV) was performed using a set of sealed radioactive sources (1 cm in diameter and about 40 kBq activity): $^{133}$Ba, $^{137}$Cs, $^{54}$Mn, $^{57}$Co, $^{109}$Cd, $^{22}$Na and $^{60}$Co. The efficiency calibration was performed with the use of a geometry of room/box with internal surface contamination, modelled in Geometry Composer software applying ISOCSTM software and monoenergetic photons covering the energy range of 10 – 3300 keV (an adequate measuring range). The monoenergetic photon flux density was estimated from the photopeak areas employing detection efficiency curve ε(E), Ge crystal surface area and lifetime of spectrum acquisition. An effective dose was estimated using photon flux-to-dose conversion coefficients for isotropic irradiation with monoenergetic photons, interpolated on the basis of data provided by the International Commission on Radiological Protection (ICRP) in report 116 using a third-degree Lagrange formula. Identification of in-situ registered radioisotopes was based on the photopeaks' energies.

## Measurements performed in free space

**Efficiency modeling**

***Horizontal orientation of spectrometer***

Geometry for efficiency calibration was based on room/box with internal surface contamination (software template) with dimensions of investigated localization. Radioactivity was assumed to be distributed equally between 5 out of 6 walls.

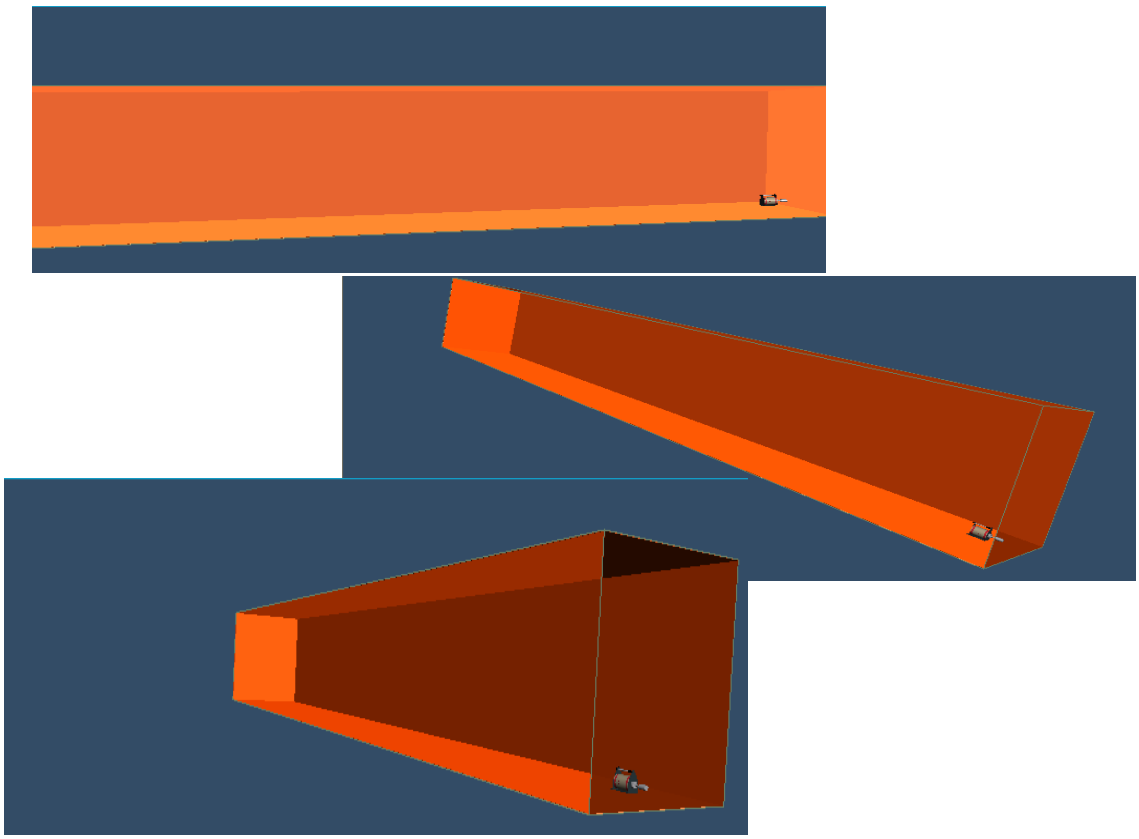

Fig. 2 The geometry for modeling the detection efficiency, obtained with the use of Geometry Composer v.4.2.1 (Canberra Industries, Inc.).

Description of detector settings during measurement (where the detector was placed (near wall, floor….):

detector position (horizontal, vertical): **horizontal position**
distance from the walls: **30 cm**
measurement of the gamma-ray spectrum from the wall, floor, concrete, other: **30 cm in front of the nearest wall (the centre of the germanium crystal was 25 cm above the floor)**
use of a collimator during the measurement (if yes, what): **no**

- Results

Tab. 2 Results of in-situ gamma-ray measurements.

| **Hall ID** (and place) | **Measurement method** | **Equipment type** | **Detection relative efficiency** [%] | **Energy range** [keV] | **Results** (integrated counts per second) [cps] |
|---|---|---|---|---|---|
| blind chamber excavation | Gamma spectroscopy | -GR4020 portable spectrometer,<br>-HPGe coaxial detector,<br>-InSpector™ 2000 multichannel -analyser (for data collecting),<br>-Genie™ 2000 v.3.2.1 software package (for spectra analysing) | 40 | 7-3150 | 350.00±0.05* |

*data are presented in A. Walencik-Łata, et al., Characteristics of Natural Background Radiation in the GIG Experimental Mine 'Barbara', Poland. Energies 2022, 15, 685

Schematic plan of the Hall with marked sites where the measurements were performed.

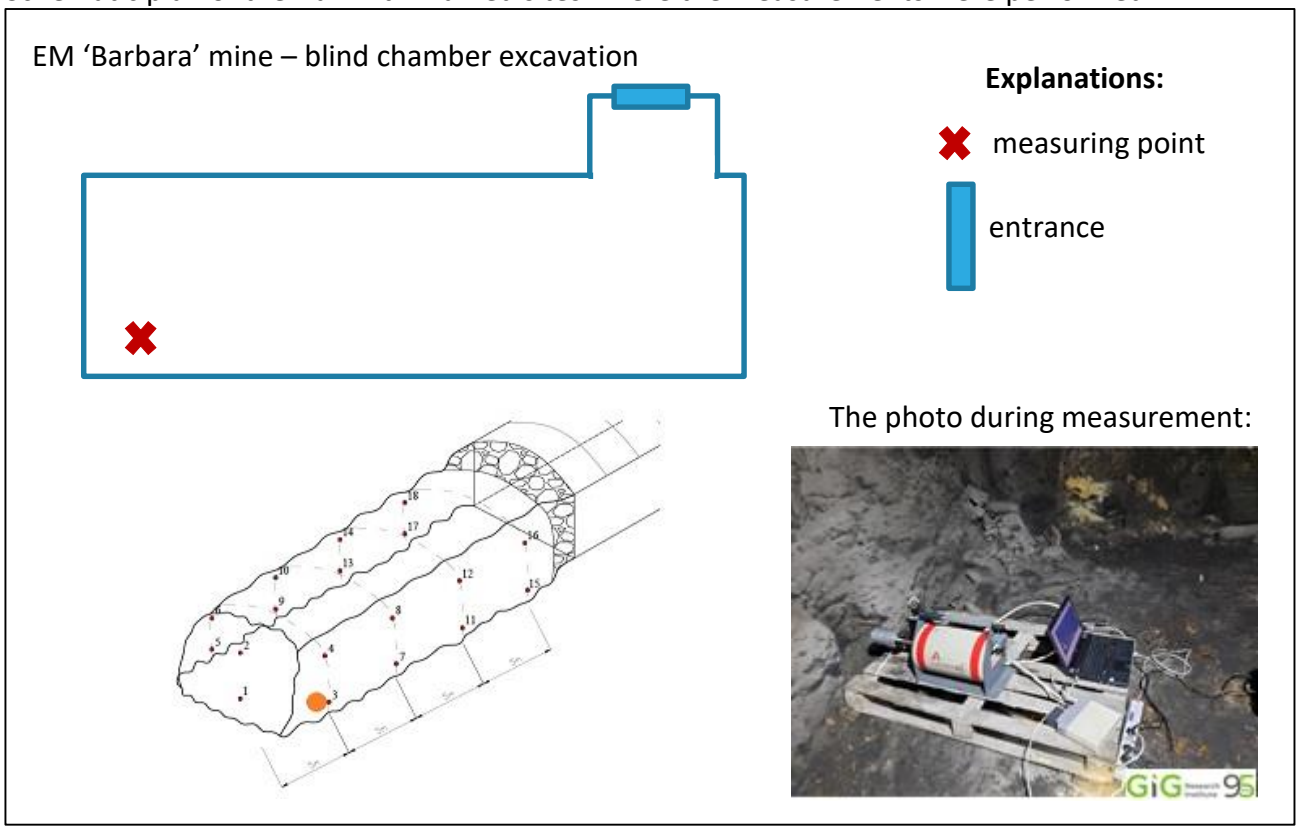


Fig. 3 Schematic plan of the blind chamber excavation with the marked site where the in-situ gamma-ray measurement was performed.

Gamma-ray spectrum:

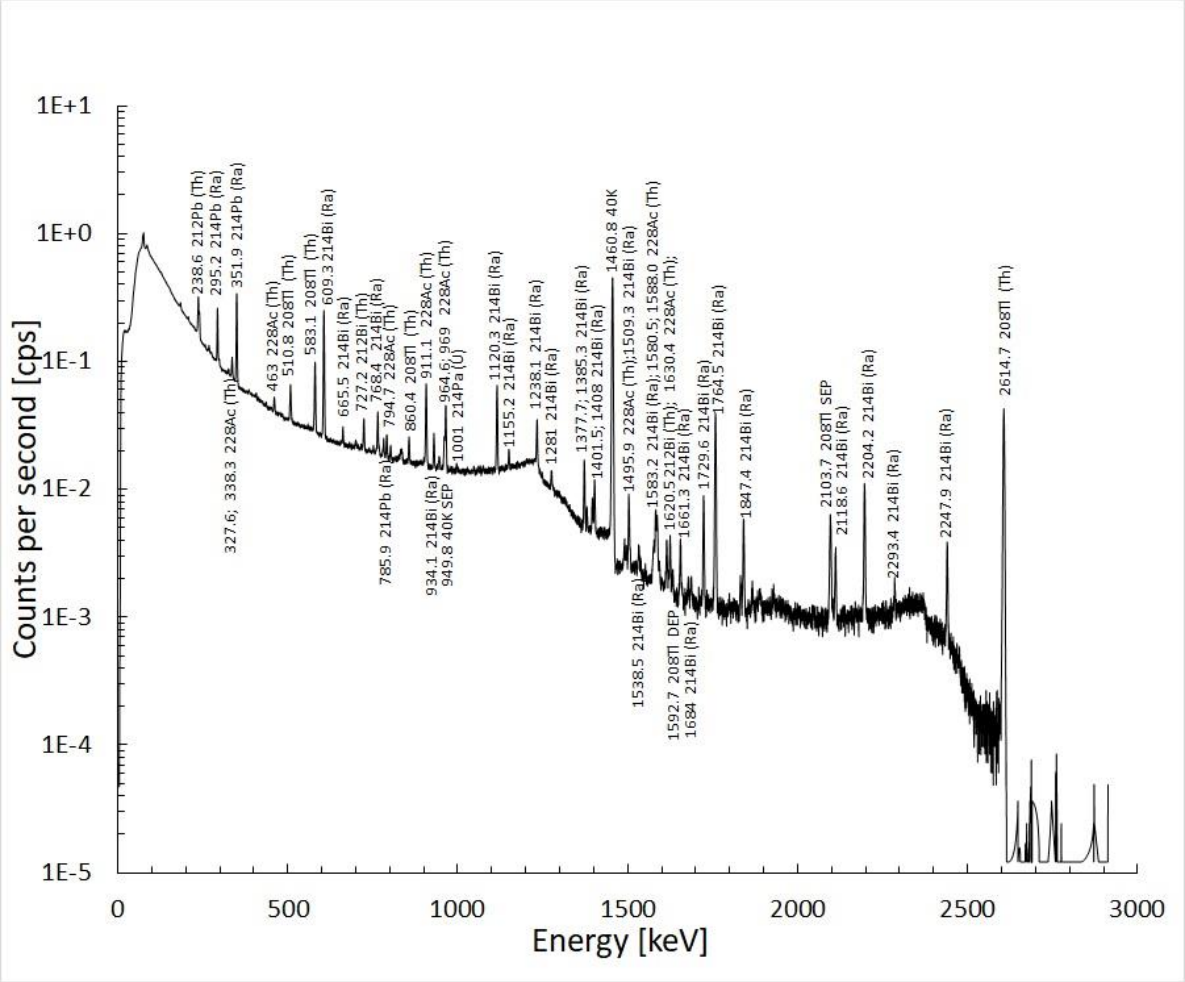


Fig. 4 Gamma-ray spectrum from a blind chamber excavation site.

Other relevant information:

Tab. 3 Results of gamma-ray flux, gamma-ray dose, and contribution of the radioisotopes for the investigated localizations.

| **Hall ID** (and place) | **Gamma flux** [$cm^{-2}s^{-1}$] | **Gamma-ray dose** [μSv/h] | **Radioisotopes that have the main contributions ineffective dose** | | |
|---|---|---|---|---|---|
| | | | **Decay chain** | **Isotope** | **Concentration** [%] |
| blind chamber excavation | 17.6 ± 1.9* | 0.200 ± 0.029* | -<br>Uranium<br>Thorium<br>Thorium<br>Uranium | $^{40}K$<br>$^{214}Bi$<br>$^{208}Tl$<br>$^{228}Ac$<br>$^{214}Pb$ | 46.7<br>25.1<br>15.2<br>6.6<br>3.3 |

*data are presented in A. Walencik-Łata, et al., Characteristics of Natural Background Radiation in the GIG Experimental Mine 'Barbara', Poland. Energies 2022, 15, 685

Qualitative analysis of gamma-ray spectra registered in underground laboratory.

Qualitative analysis of gamma ray spectra registered in underground laboratory (LT - live time, measuring time; Area – net area of the photopeak on the spectrum gamma ray)
(SEP – single escape peak, DEP – double escape peak)

Tab. 4 Qualitative analysis of gamma-ray spectrum registered in EM 'Barbara' mine – blind chamber excavation.

| True Energy [keV] | Isotope | CPS = Area/LT | Δ CPS |
|---|---|---|---|
| 12.97 | X: Th $L_{\alpha 1}$ | 0.2643 | 0.0054 |
| 46.5 | $^{210}$Pb | 0.2510 | 0.0099 |
| 51.62 | $^{239}$Pu | 0.1364 | 0.0106 |
| 74.97 | X:Pb $K_{\alpha 1}$ | 1.1055 | 0.0297 |
| 77.12 | X:Bi $K_{\alpha 1}$ | 2.3414 | 0.0349 |
| 87.34 | X:Bi $K_{\beta 1}$ | 0.8424 | 0.0156 |
| 92.59 | $^{234}$Th | 0.3343 | 0.0133 |
| 129.07 | $^{228}$Ac | 0.1179 | 0.0151 |
| 186.1 | $^{226}$Ra | 0.2052 | 0.0131 |
| 209.25 | $^{228}$Ac | 0.1019 | 0.0111 |
| 238.63 | $^{212}$Pb | 1.1381 | 0.0072 |
| 241.98 | $^{214}$Pb | 0.6409 | 0.0061 |
| 258.87 | $^{214}$Pb | 0.0448 | 0.0096 |
| 270.24 | $^{228}$Ac | 0.1196 | 0.0054 |
| 277.35 | $^{208}$Tl | 0.0661 | 0.0049 |
| 295.21 | $^{214}$Pb | 1.0995 | 0.0057 |
| 300.09 | $^{212}$Pb | 0.0968 | 0.0037 |
| 327.6 | $^{228}$Ac | 0.0673 | 0.0072 |
| 338.32 | $^{228}$Ac | 0.2643 | 0.0088 |
| 351.92 | $^{214}$Pb | 1.9431 | 0.0098 |
| 387.0 | $^{214}$Bi | 0.0279 | 0.0069 |
| 409.46 | $^{228}$Ac | 0.0299 | 0.0058 |
| 438.83 | $^{40}$K (DEP) | 0.0163 | 0.0057 |
| 463.01 | $^{228}$Ac | 0.0996 | 0.0062 |
| 480.43 | $^{214}$Pb | 0.0093 | 0.0023 |
| 487.08 | $^{214}$Pb | 0.0135 | 0.0025 |
| 510.77 | $^{208}$Tl | 0.2703 | 0.0064 |
| 562.5 | $^{228}$Ac | 0.0170 | 0.0046 |
| 583.19 | $^{208}$Tl | 0.5853 | 0.0065 |
| 609.31 | $^{214}$Bi | 1.6776 | 0.0074 |
| 665.45 | $^{214}$Bi | 0.0474 | 0.0022 |

| | | | |
|---|---|---|---|
| 703.11 | $^{214}$Bi | 0.0203 | 0.0045 |
| 719.86 | $^{214}$Bi | 0.0142 | 0.0019 |
| 727.2 | $^{212}$Bi | 0.1291 | 0.0026 |
| 755.32 | $^{228}$Ac | 0.0121 | 0.0044 |
| 768.36 | $^{214}$Bi | 0.1678 | 0.0055 |
| 785.91 | $^{214}$Pb | 0.0520 | 0.0020 |
| 794.95 | $^{228}$Ac | 0.0752 | 0.0021 |
| 806.17 | $^{214}$Bi | 0.0413 | 0.0019 |
| 835.71 | $^{228}$Ac | 0.0210 | 0.0019 |
| 839.03 | $^{214}$Pb | 0.0280 | 0.0021 |
| 860.56 | $^{208}$Tl | 0.0771 | 0.0046 |
| 911.21 | $^{228}$Ac | 0.4369 | 0.0056 |
| 934.06 | $^{214}$Bi | 0.1020 | 0.0048 |
| 949.83 | $^{40}$K (SEP) | 0.0311 | 0.0042 |
| 964.77 | $^{228}$Ac | 0.0947 | 0.0020 |
| 968.97 | $^{228}$Ac | 0.2595 | 0.0027 |
| 1001.03 | $^{234}$Pa | 0.0093 | 0.0029 |
| 1051.96 | $^{214}$Bi | 0.0115 | 0.0037 |
| 1069.96 | $^{214}$Bi | 0.0084 | 0.0015 |
| 1078.62 | $^{212}$Bi | 0.0089 | 0.0015 |
| 1120.29 | $^{214}$Bi | 0.4043 | 0.0029 |
| 1133.66 | $^{214}$Bi | 0.0038 | 0.0016 |
| 1155.19 | $^{214}$Bi | 0.0482 | 0.0039 |
| 1238.11 | $^{214}$Bi | 0.1641 | 0.0048 |
| 1253.5 | $^{214}$Bi (SEP) | 0.0046 | 0.0029 |
| 1280.98 | $^{214}$Bi | 0.0339 | 0.0036 |
| 1377.67 | $^{214}$Bi | 0.0980 | 0.0016 |
| 1385.31 | $^{214}$Bi | 0.0197 | 0.0010 |
| 1401.5 | $^{214}$Bi | 0.0336 | 0.0012 |
| 1407.98 | $^{214}$Bi | 0.0618 | 0.0014 |
| 1460.83 | $^{40}$K | 4.2242 | 0.0077 |
| 1495.9 | $^{228}$Ac | 0.0127 | 0.0008 |
| 1501.577 | $^{228}$Ac | 0.0078 | 0.0008 |
| 1509.23 | $^{214}$Bi | 0.0555 | 0.0012 |
| 1538.5 | $^{214}$Bi | 0.0138 | 0.0009 |
| 1543.32 | $^{214}$Bi | 0.0069 | 0.0007 |
| 1580.54 | $^{228}$Ac | 0.0224 | 0.0009 |
| 1588.21 | $^{228}$Ac | 0.0506 | 0.0012 |
| 1592.53 | $^{208}$Tl (DEP) | 0.0420 | 0.0011 |
| 1599.31 | $^{214}$Bi | 0.0092 | 0.0007 |
| 1620.5 | $^{212}$Bi | 0.0220 | 0.0008 |
| 1630.63 | $^{228}$Ac | 0.0255 | 0.0008 |

| | | | |
|---|---|---|---|
| 1638.28 | $^{228}$Ac | 0.0088 | 0.0007 |
| 1661.28 | $^{214}$Bi | 0.0259 | 0.0018 |
| 1683.99 | $^{214}$Bi | 0.0053 | 0.0006 |
| 1693.21 | $^{214}$Bi (DEP) | 0.0073 | 0.0007 |
| 1729.6 | $^{214}$Bi | 0.0669 | 0.0011 |
| 1764.5 | $^{214}$Bi | 0.3440 | 0.0026 |
| 1838.36 | $^{214}$Bi | 0.0079 | 0.0006 |
| 1847.42 | $^{214}$Bi | 0.0426 | 0.0009 |
| 1873.16 | $^{214}$Bi | 0.0087 | 0.0015 |
| 2052.94 | $^{214}$Bi | 0.0031 | 0.0009 |
| 2103.5 | $^{208}$Tl (SEP) | 0.0599 | 0.0010 |
| 2118.55 | $^{214}$Bi | 0.0253 | 0.0008 |
| 2204.21 | $^{214}$Bi | 0.0957 | 0.0019 |
| 2293.36 | $^{214}$Bi | 0.0097 | 0.0015 |
| 2447.86 | $^{214}$Bi | 0.0286 | 0.0013 |
| 2614.7 | $^{208}$Tl | 0.4453 | 0.0024 |
| 2769.9 | $^{214}$Bi | 0.0003 | 0.0001 |
| 2880.3 | $^{214}$Bi | 0.0002 | 0.0001 |
| 2978.9 | $^{214}$Bi | 0.0003 | 0.0001 |

Apparent radioactivity and effective dose rate calculated on the base of the gamma-ray spectrum.

*Tab. 5 Effective dose rate and apparent radioactivity results calculated based on the gamma-ray spectrum for blind chamber excavation site*.*

| Decay chain | Radionuclide | Effective dose rate [pSv/s] | % contribution | Apparent activity in measuring point [Bq/cm$^2$] |
|---|---|---|---|---|
| Uranium | $^{234}$Th | 0.025 ± 0.004 | 0.05 | 3.36 ± 0.59 |
| Thorium | $^{228}$Ac | 3.66 ± 0.54 | 6.6 | 1.45 ± 0.40 |
| Uranium | $^{226}$Ra | 0.036 ± 0.006 | 0.06 | 1.89 ± 0.42 |
| Thorium | $^{212}$Pb | 0.342 ± 0.049 | 0.61 | 1.12 ± 0.21 |
| Uranium | $^{214}$Pb | 1.85 ± 0.27 | 3.32 | 2.55 ± 0.51 |
| Thorium | $^{208}$Tl | 8.43 ± 1.23 | 15.16 | 0.63 ± 0.18 |
| Uranium | $^{214}$Bi | 13.97 ± 2.07 | 25.13 | 3.26 ± 0.38 |
| Thorium | $^{212}$Bi | 0.571 ± 0.085 | 1.03 | 1.92 ± 0.23 |
| Uranium | $^{234m}$Pa | 0.032 ± 0.011 | 0.06 | 1.23 ± 0.40 |
| | $^{40}$K | 26.06 ± 3.70 | 46.88 | 51.63 ± 5.10 |
| | $^{239}$Pu | 0.011 ± 0.002 | 0.02 | 19.00 ± 5.06 |
| Uranium: | $^{210}$Pb | 0.018 ± 0.003 | 0.03 | 2.45 ± 0.34 |
| | X rays | 0.343 ± 0.049 | 0.62 | |

| | | | | |
|---|---|---|---|---|
| | annihilation | 0.242 ± 0.035 | 0.44 | |

*data are presented in A. Walencik-Łata, et al., Characteristics of Natural Background Radiation in the GIG Experimental Mine 'Barbara', Poland. Energies 2022, 15, 685

### *b. Measurements of the radon concentration in air*

- Information about measurement

Measurements of the radon concentration in the air were performed using the RAD7 radon detector. The measurements were made in cycles.

Description of detector settings during measurement (where the detector was placed (near wall, floor….):
Place of the measurement: **in blind chamber excavation, detector was located opposite/near the gamma-ray spectrometer – right corner**
Ventilation (on/off): **ventilation on and off**
Other relevant information (use a drying unit, humidity, temperature, pressure, other):
**measurement was performed with use a drying unit, humidity 70%, temperature *12°C***

- Results

Tab. 6 The results of radon concentration in the air at the EM 'Barbara' mine – blind chamber excavation.

| **Hall ID** | **Measurement method** | **Equipment type** | **Collection period** | **Average result** [Bq/m$^3$] |
|---|---|---|---|---|
| blind chamber excavation | Alpha spectroscopy | RAD7 electronic radon detector (Durridge), | 9 days (0.5 - 1 h-long each) | 205-34300 (depending on the ventilation of the chamber) |

Schematic plan of the Hall with marked sites where the measurements were performed.

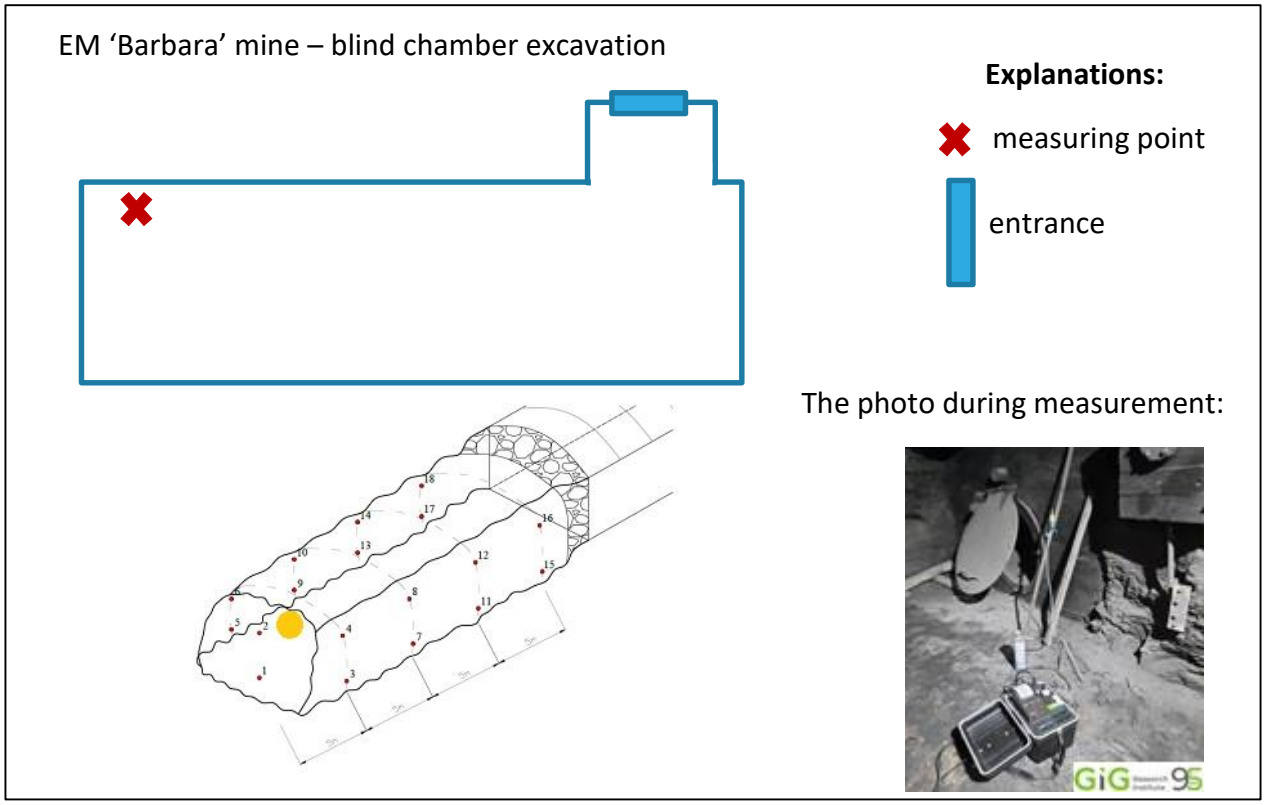


Fig. 5 Schematic plan of the blind chamber excavation site with the marked sites where the measurements of the radon concentration in air were performed.

Plot of radon activity concentration in blind chamber excavation.

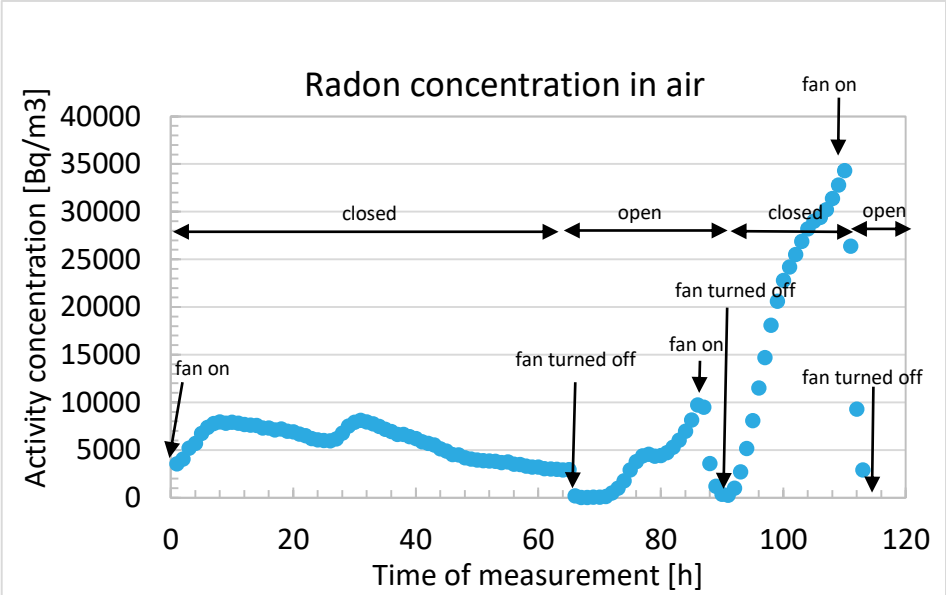


Fig. 6 Plot of radon concentration in the air in EM 'Barbara' mine – blind chamber excavation.

### *c.* Measurements *of the neutron flux*

- Information about measurement

The thermal neutron flux was measured using helium counters, i.e., gas proportional counters filled with helium-3 ($^3$He). In this type of detector, neutrons are captures by helium nucleus in the reaction: $^3He(n,p)^3H$ + 764 keV and the charged products (proton and Tritium) of the reaction appear with kinetic energy 764 keV. This method allows distinguishing neutrons events even with a large background of other types of radiation. The setup consisted of a flat tray of helium counters positioned vertically in a rack, four Centronic counters, and four ZDAJ counters. The data acquisition system (DAQ) was designed and made in NCBJ-Łódź laboratory. DAQ is built in the form of a cassette with eight measurement cards. Each card contains four independent measurement channels, up to 32 input channels in total. Each measurement channel is sampled with a frequency of 10 MHZ by an ADC with a dynamic of 10 bits. DAQ contains a built-in Raspberry Pi computer. Therefore it works as an autonomous system, without the need to connect to an external computer. The analyze the pulse shape (PSD) was applied. PSD allows rejecting disturbances. The PSD analysis was based on the two-dimensional distribution of the maximum pulse amplitude versus the maximum pulse jump on the rising edge.

*Standard method:*

a) Type of counters (helium/boron) and name of the manufacturer, counter's dimensions: **proportional $^3$He counters, Centronic counters (Centronic 50He3/190/50MS), ZDAJ counters (ZDAJ NEM425A50). The counters of both types were steel pipes 50 cm long, but they differed in diameter (5 cm for Centronic and 2.5 cm for ZDAJ) and helium-3 pressure (2 atm for Centronic and 4 atm for ZDAJ).**

b) Setup description: number of counters, their distances in a tray etc.:
**A flat tray of helium counters was positioned vertically in a rack. The tray was divided into two parts: first, there were four Centronic counters, then there was a 30 cm space, and again four ZDAJ counters. There were 5 cm gaps between the individual counters.**

c) Place of measurement: chamber name, distance from walls, large objects nearby and what they are made of (water, polyethylene, graphite, etc.): **detection setup for the neutron measurements was placed in the center of blind chamber excavation, a distance few cm from walls**
d) Humidity: normal / low / high

- Results

Tab. 7 Results of the neutron flux measurements.

| Hall ID | Collection period | Average neutron counting rate | Dispersion of neutron counting rate | Calculated neutron flux witch error |
|---|---|---|---|---|
| blind chamber excavation | 2 weeks | 16.6 ± 2.8 (for Centronic) and 6.8±1.2 (for ZDAJ) neutrons per hour* | | $(8.6\pm1.1)\cdot10^{-6}$ $[cm^{-2}s^{-1}]$* |

*data are presented in A. Walencik-Łata, et al., Characteristics of Natural Background Radiation in the GIG Experimental Mine 'Barbara', Poland. Energies 2022, 15, 685

Schematic plan of detector location in the blind chamber excavation.

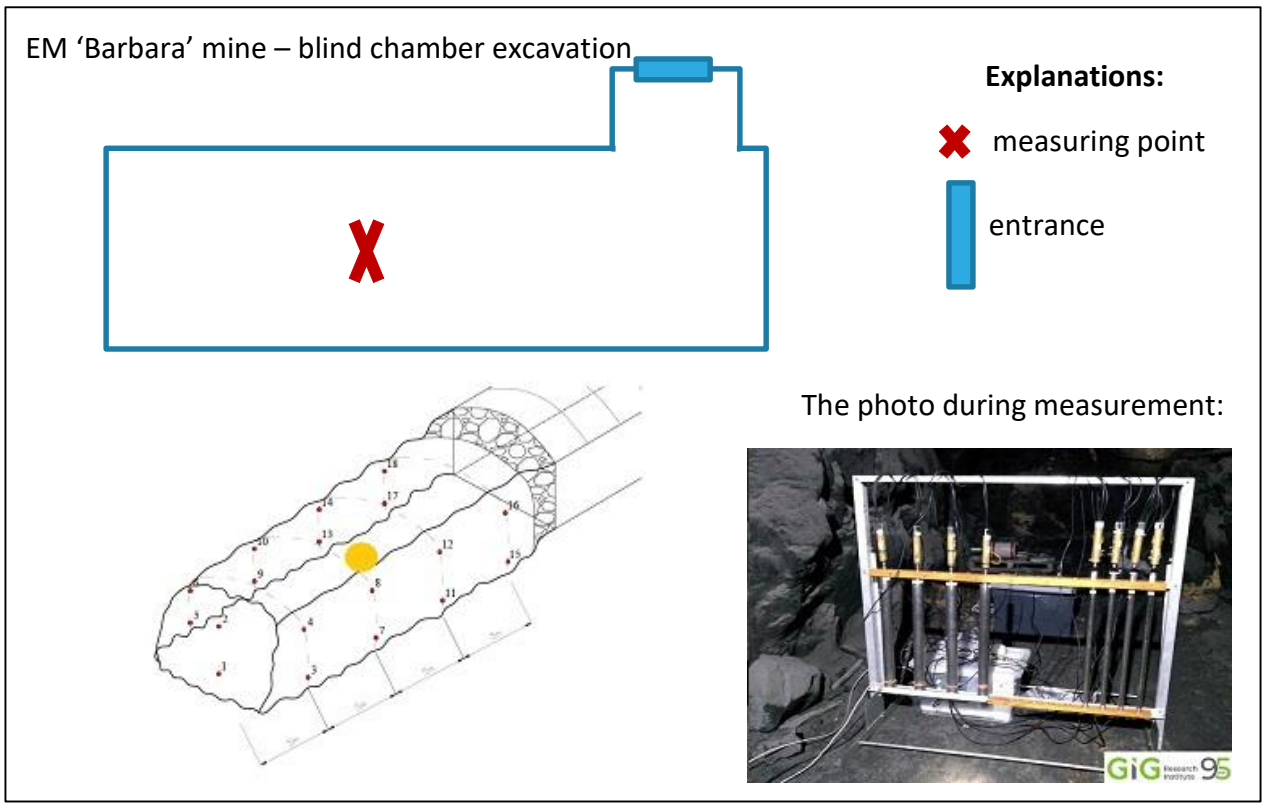


Fig. 7 Schematic plan of neutron detector located in the blind chamber excavation.

Distribution of amplitude of signals from $^{3}$He counter:

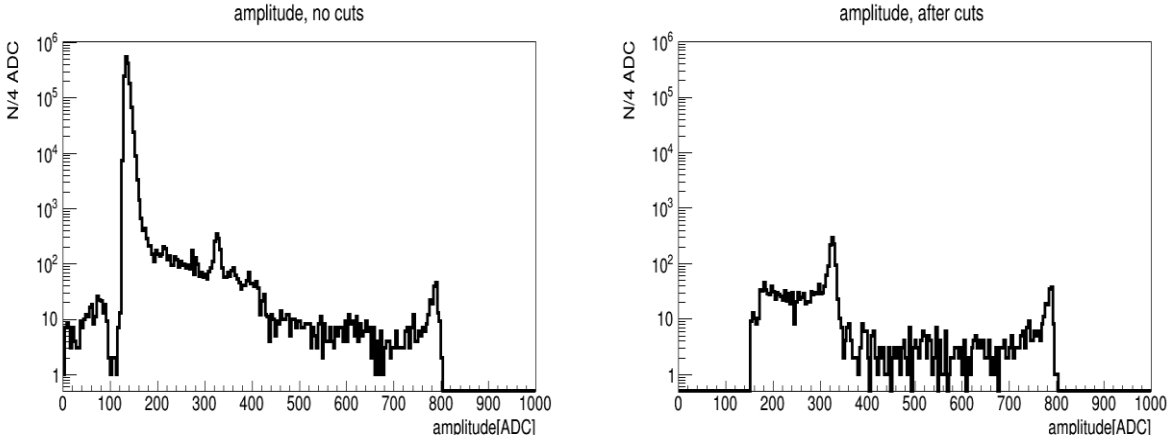


Fig. 8 The recorded spectrum of amplitudes before and after the application cuts.

## 3. Laboratory analyses of the water samples

Measurements of the concentration of radium and uranium radioisotopes in water samples were carried out in an external laboratory - "Low-level Activity Research Laboratory", Institute of Physics, the University of Silesia in Katowice, Poland.

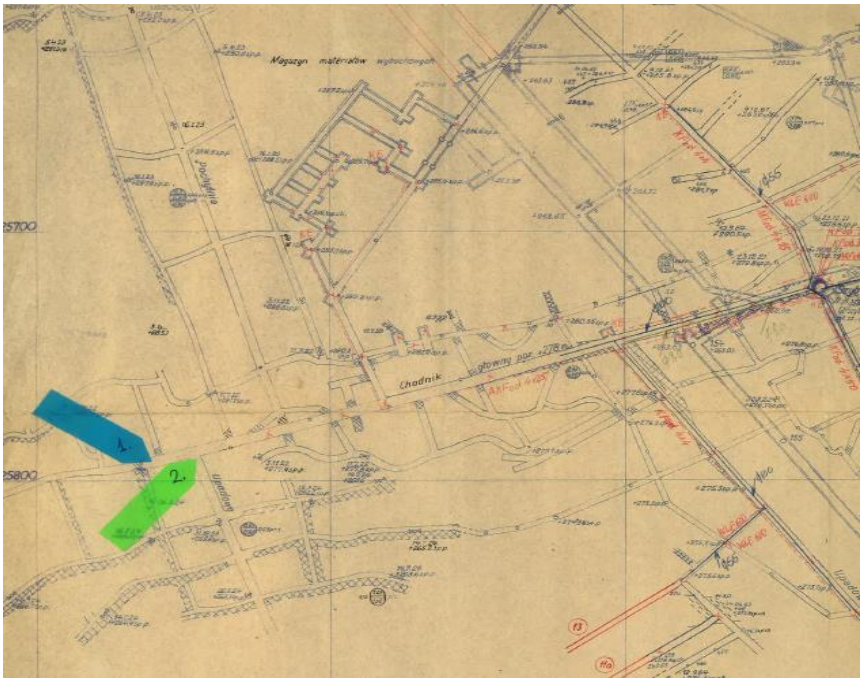


**Fig. 9 Diagram of the 30 m level, layer 310, where water, sediment, carbon, stone, slate, and sandstone samples were collected for laboratory analysis. Part one.**

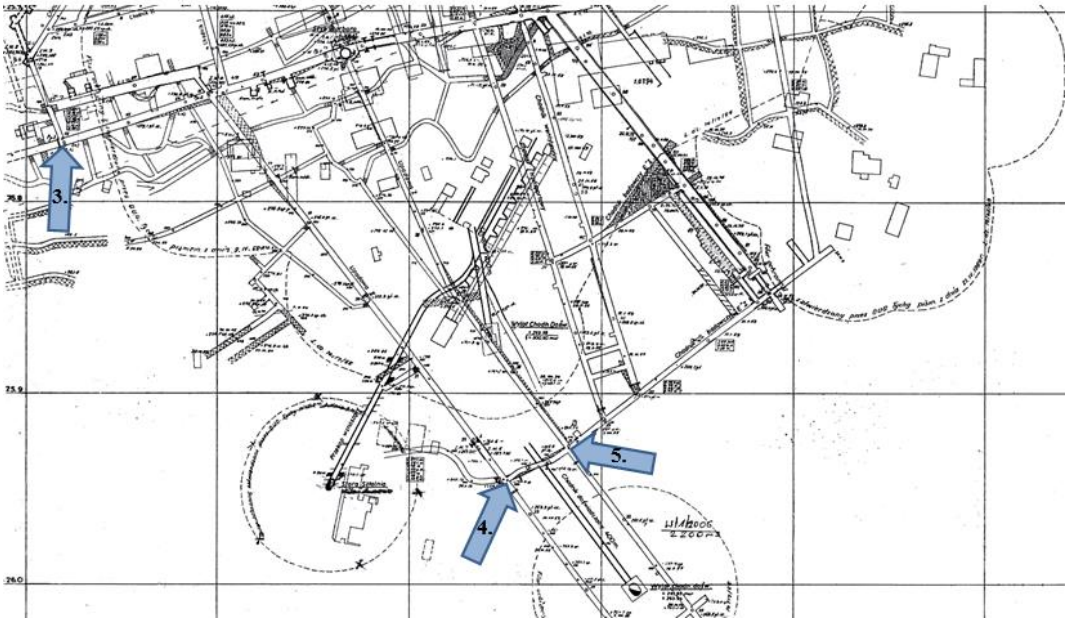


Fig. 10 Diagram of the 30 m level, layer 310, where water, sediment, carbon, stone, slate, and sandstone samples were collected for laboratory analysis. Part two.

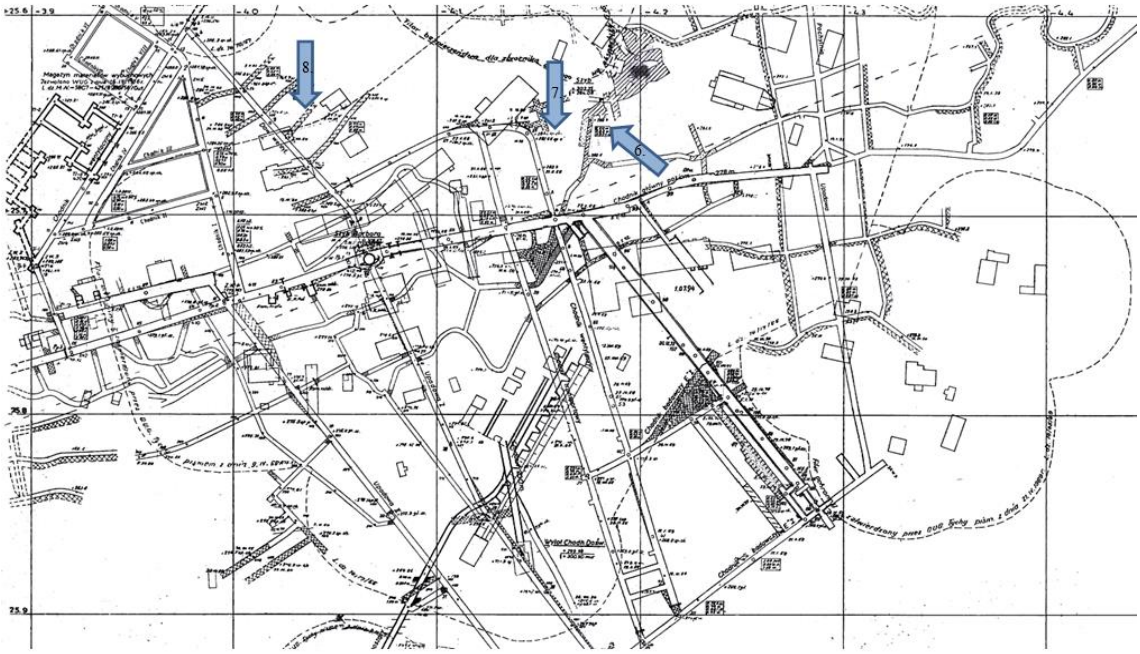


Fig. 11 Diagram of the 30 m level, layer 310, where water, sediment, carbon, stone, slate, and sandstone samples were collected for laboratory analysis. Part three.

Description of the sites where water samples were taken:

Tab. 8 Description of the sites where water samples were collected.

| **Hall ID** | **Depth below surface** [m w.e.] | **Sites** (wall, water gullets, water reservoir, other…..) | **Method of the sampling** |
|---|---|---|---|
| Localization 1 - water sample 1 | 80 (layer 310) | water gullets, stagnant water | Sampling for polyethylene bottles |
| Localization 2 - water sample 1,2bis | | | |
| Localization 3 - water sample 3 | | | |
| Localization 4 - water sample 4 | | | |
| Localization 5 - water sample 5 | | | |
| Localization 6 - water sample 6 | | | |
| Localization 8 - water sample 8 | | | |

The samples were acidified immediately after collection to avoid precipitation of radionuclides and adsorption on the walls of the containers.

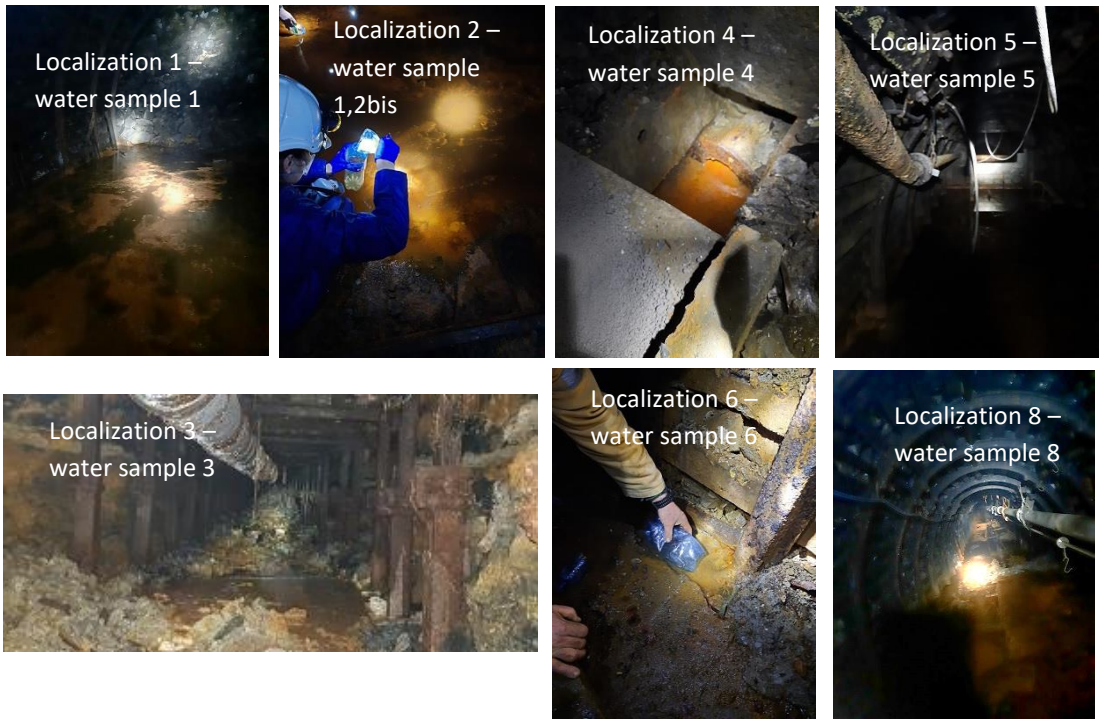


Fig. 12 Water sampling site from EM 'Barbara'.

### *a. Uranium concentration in water samples*

- Description of the performed chemical procedure

The concentration of uranium $^{234}U$ and $^{238}U$ isotopes in the water samples were determined by semiconductor alpha spectrometry using a 7401VR spectrometer (Canberra, USA) and an Alpha Analyst™ (Mirion Technologies (Canberra), Inc., USA) (**Fig. *13***). A radiochemical procedure was applied to prepare an alpha spectrometric source before measurement. The samples were acidified with $HNO_3$ and spiked with a known amount of $^{232}U$. The separation of U is performed using anion exchange resin Dowex 1×8 (Cl- type, 200-400 mesh) based on a procedure worked out by Suomela (1993). The spectrometric source was prepared by co-precipitation of U with $NdF_3$ and deposition on polypropylene disks (0.1 µm) (Pall Corporation).

References:
J. Suomela, Method for determination of U-isotopes in water, Swedish Radiation Institute, Stockholm, SSI-rapport, 0282-4434, 93:14 (1993).

(a) 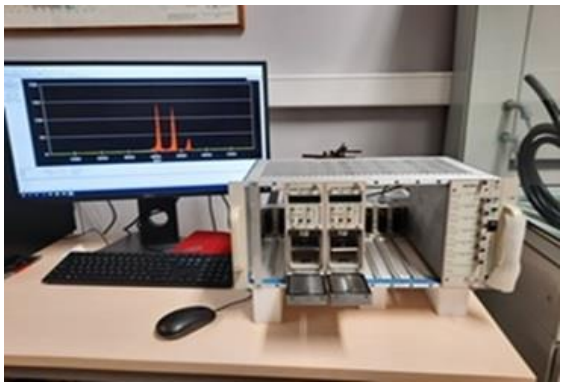 (b) 


**Fig. 13 (a) the spectrometer 7401VR (Canberra, USA), (b) the alpha spectrometer Alpha Analyst™ (Mirion Technologies (Canberra), Inc., USA).**

- Information about measurement and results

Tab. 9 Results of uranium radioisotopes concentration in water samples from EM 'Barbara'.

| Hall ID (name of the sample) | Measu-rement method | Equipment type | Collection period | Limit of detection | Average results [mBq/l] | | ratio $^{234}U/^{238}U$ | U [µg/l] |
|---|---|---|---|---|---|---|---|---|
| | | | | | $^{234}U$ | $^{238}U$ | | |
| Water sample loc.1 | Alpha spectro-scopy | spectrometer 7401VR (Canberra, USA) | 2-7 days | 0.5 mBq/l for $^{234,238}U$, 0.5 l initial sample volume | 3.3±0.3 | 2.4±0.2 | 1.39±0.16 | 0.19±0.02 |
| Water sample loc.1,2bis | | | | | 3.9±0.2 | 2.3±0.2 | 1.70±0.18 | 0.18±0.02 |
| Water sample loc.3 | | | | | 35.4±0.9 | 27.7±0.8 | 1.28±0.05 | 2.24±0.06 |
| Water sample loc.4 | | | | | 5.0±0.3 | 3.7±0.3 | 1.34±0.12 | 0.30±0.02 |
| Water sample loc.5 | | | | | 2.2±0.2 | 1.0±0.1 | 2.14±0.35 | 0.08±0.01 |
| Water sample loc.6 | | | | | 6.2±0.4 | 4.6±0.4 | 1.36±0.14 | 0.37±0.03 |
| Water sample loc.8 | | | | | 1.7±0.1 | 0.7±0.1 | 2.54±0.46 | 0.06±0.01 |

Alpha spectrum:

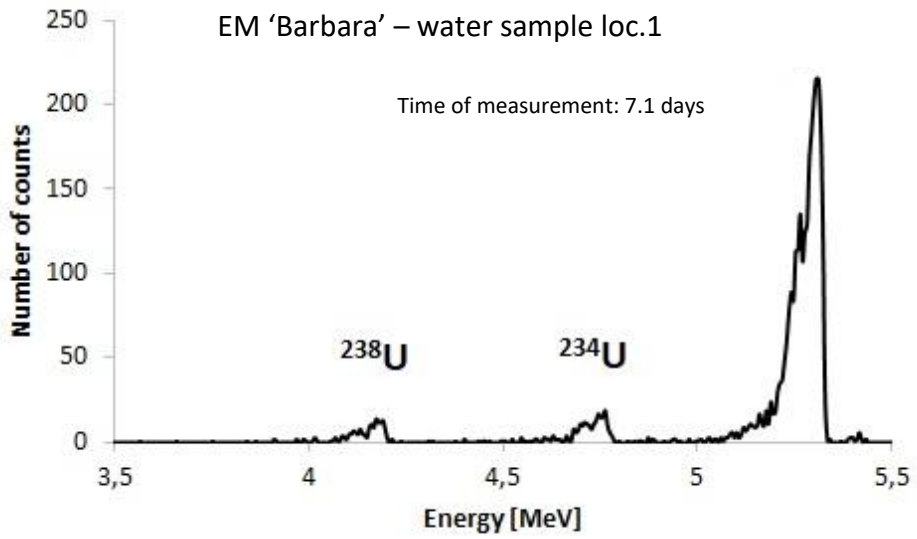


Fig. 14 The alpha spectrum of a water sample – EM 'Barbara'- water sample loc.1.

EM ‘Barbara’ – water sample loc.1,2bis

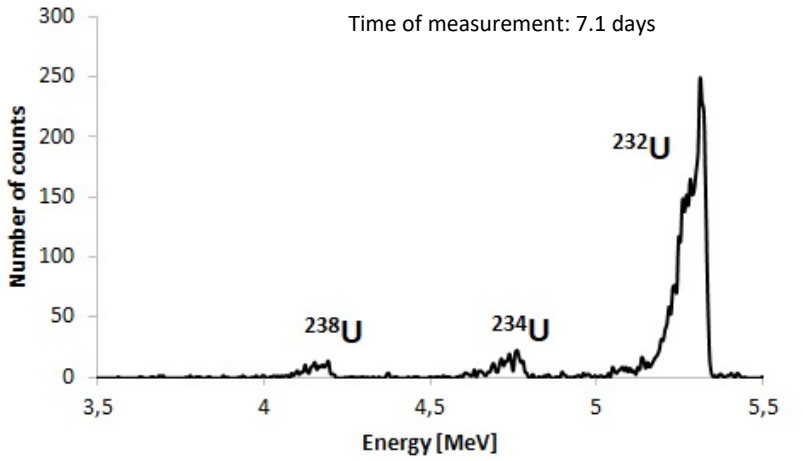


Fig. 15 The alpha spectrum of a water sample – EM ‘Barbara’- water sample loc.1,2bis.

EM ‘Barbara’– water sample loc.3

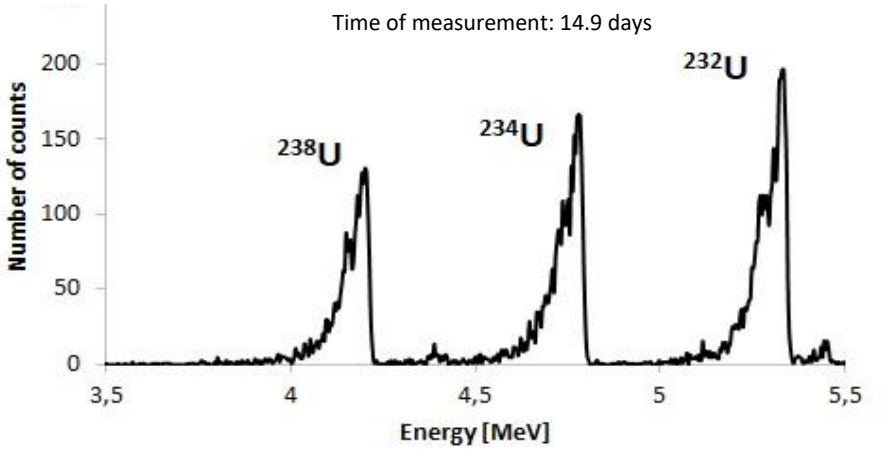


Fig. 16 The alpha spectrum of a water sample – EM ‘Barbara’ - water sample loc.3.

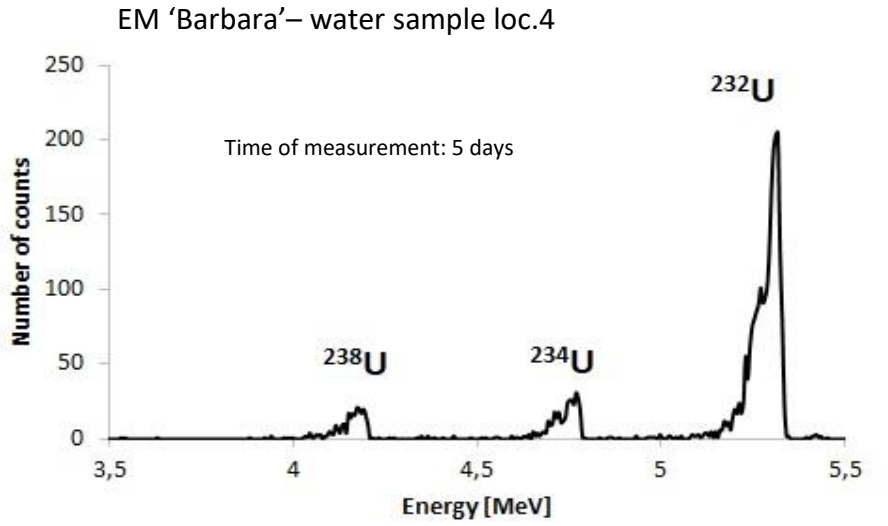


Fig. 17 The alpha spectrum of a water sample – EM 'Barbara' - water sample loc.4.

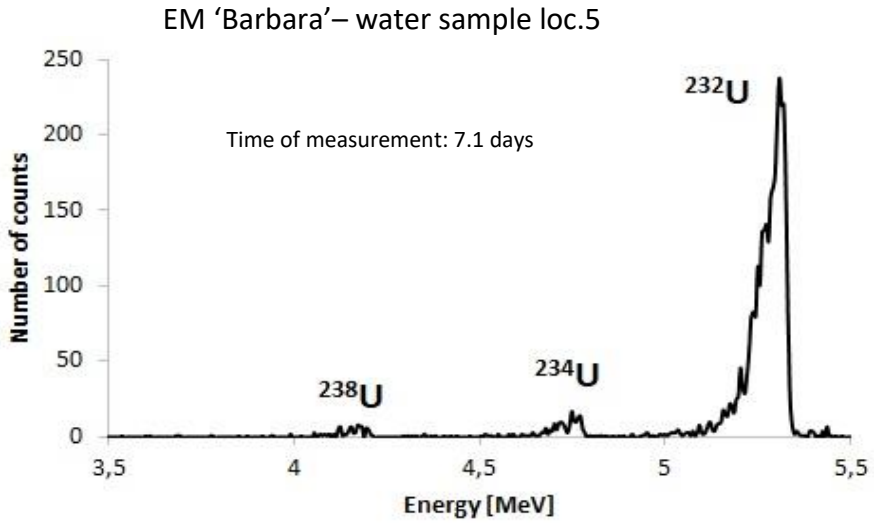


Fig. 18 The alpha spectrum of a water sample – EM 'Barbara' - water sample loc.5.

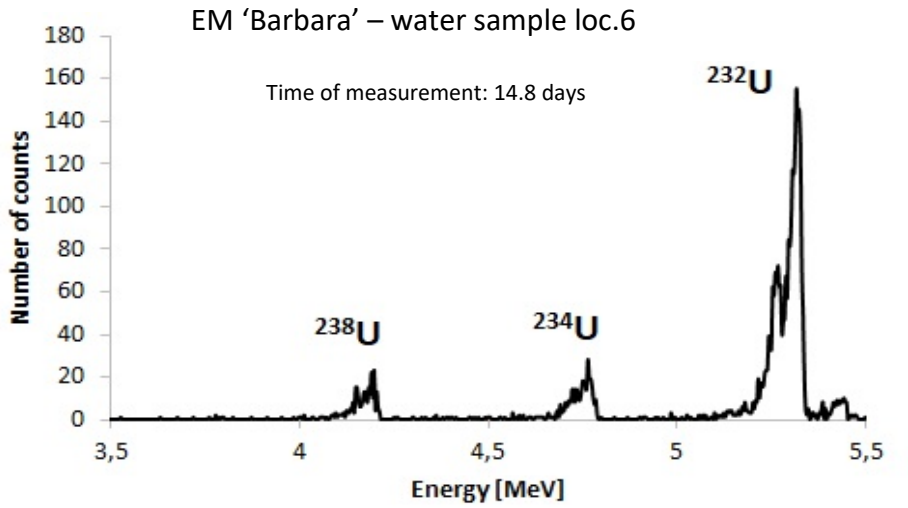


Fig. 19 The alpha spectrum of a water sample – EM 'Barbara'- water sample loc.6.

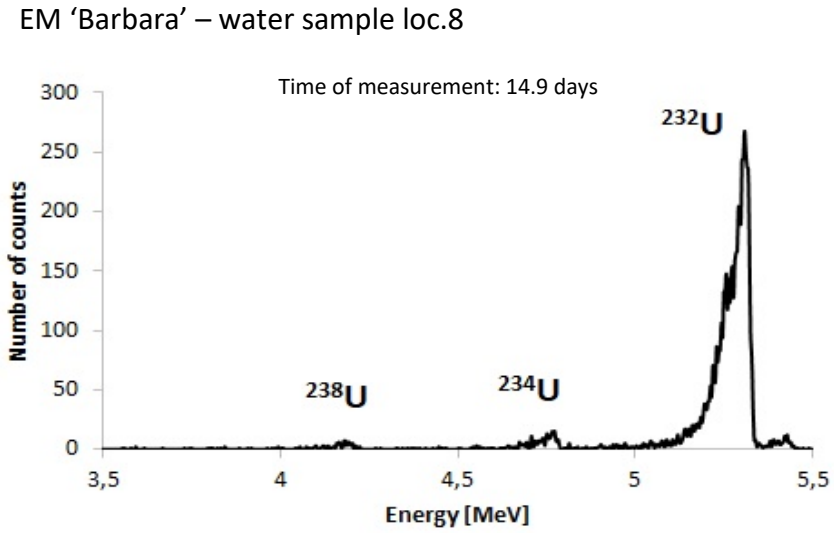


Fig. 20 The alpha spectrum of a water sample – EM 'Barbara'- water sample loc.8.

## *4.* Laboratory analyses of the rock samples

Measurements of the concentration of uranium, radium and potassium radioisotopes in the rock samples (***Fig. 21***) were performed in an external laboratory - "Low-level Activity Research Laboratory", Institute of Physics, the University of Silesia in Katowice, Poland.

Description of the sites where rock samples were taken:

Tab. 10 Description of the sites where rock samples were collected.

| **Hall ID** | **Depth below surface** [m w.e.] | **Sites** (wall, floor, brick, concrete, other) | **Method of the sampling** | **Name of the sample** |
|---|---|---|---|---|
| blind chamber excavation | 122 | wall | newly chipped rock samples from walls | Sample 1-18 |
| Localization 1 | 80 (layer 310) | | | Stone sample loc. 1 |
| Localization 2 | | | | Stone sample loc. 2 |
| Localization 2 | | | | Carbon sample loc. 2 |
| Localization 6 | | | | Slate sample loc. 6 |
| Localization 6 | | | | Sandstone sample loc. 6 |
| Localization 7 | | | | Carbon sample loc. 7 |

(a)

(b)

(c)

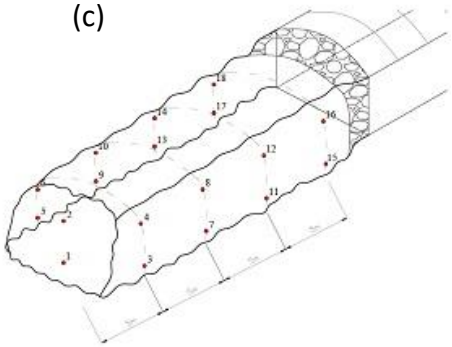

Fig. 21 (a) place of rock sampling and in-situ measurements in the EM 'Barbara' (sample 1-18), (b) approximate sampling location, (c) diagram of the place where the samples were taken.

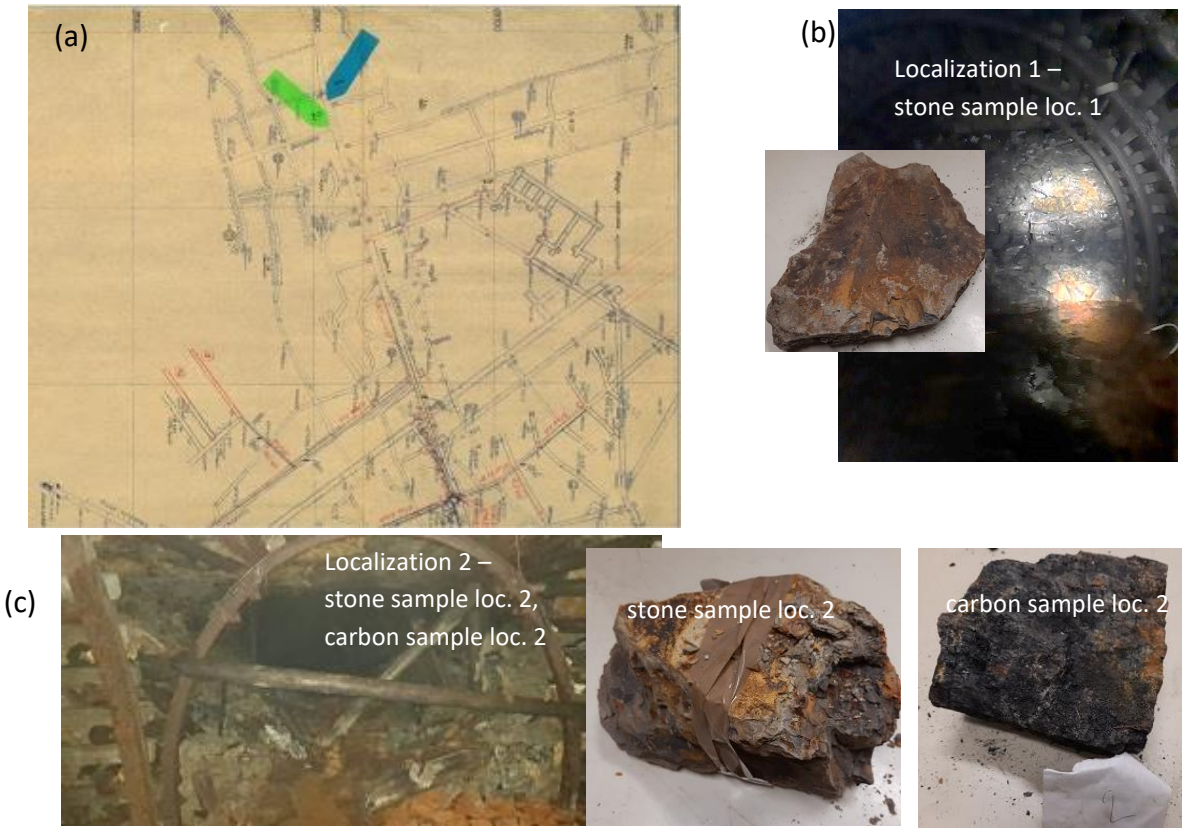


**Fig. 22 (a) diagram of the place where the samples were taken (b) localization 1 - stone sampling, (c) localization 2 – stone and carbon sampling.**

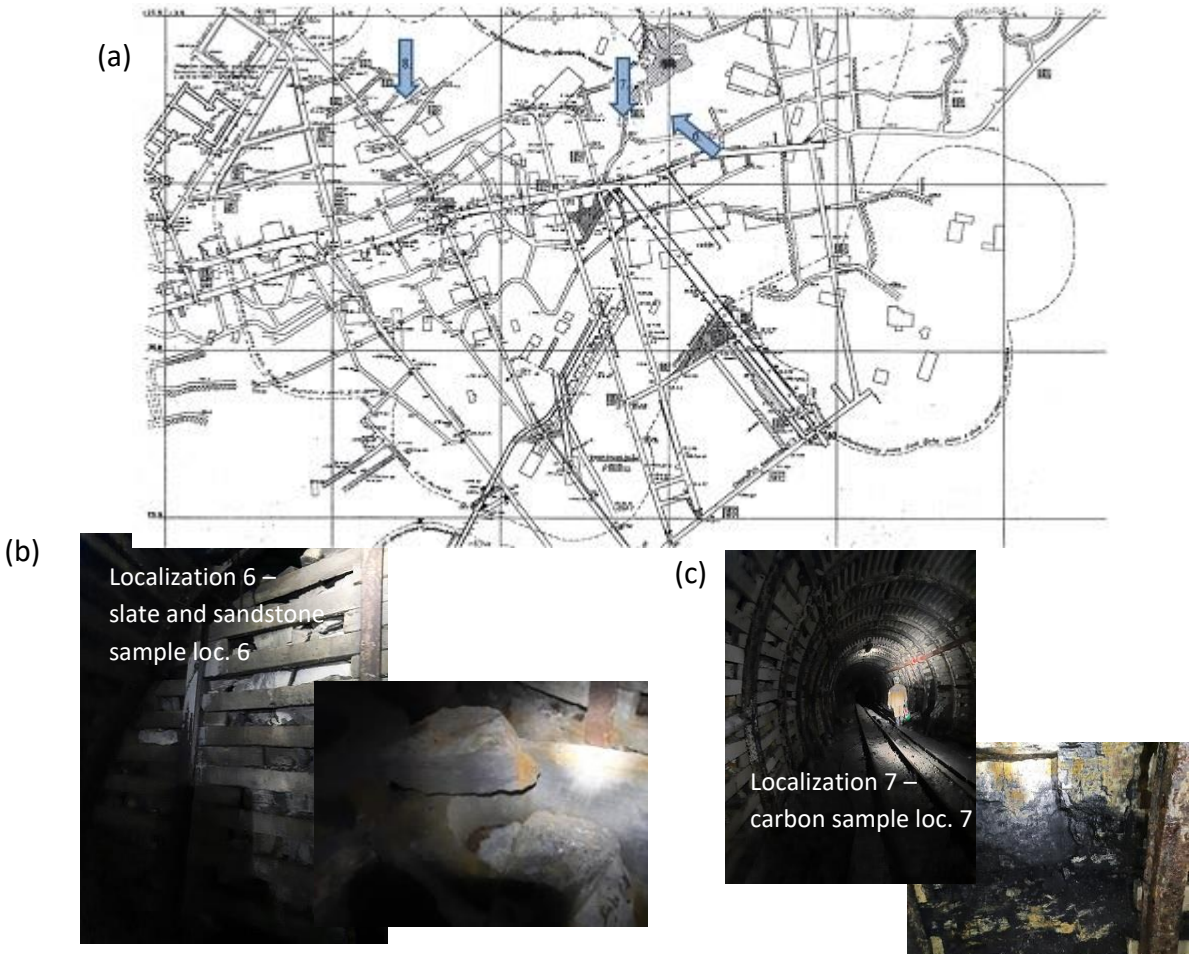


Fig. 23 (a) diagram of the place where the samples were taken (b) localization 6 – slate and sandstone sampling, localization 7 – carbon sampling.

### *a. Radium and potassium concentration in rock samples*

- Information about measurement

The concentration of radium and potassium isotopes in the rock samples was determined by gamma spectroscopy with the HPGe detector in a lead shield (***Fig. 24a***). The activity of $^{40}$K was calculated directly from a single 1460.8 keV line. The activity of $^{226}$Ra was calculated as the weighted mean of the values obtained from the $^{214}$Pb (295.2, 351.9 keV) and $^{214}$Bi (609.3, 1120.3 keV) isotopes, while $^{228}$Ra activity was calculated from the gamma lines 338.3 keV and 911.1 keV originating from $^{228}$Ac decay. The total duration of a single measurement depended on the sample activity.

Description of the procedure performed before measurements and conditions during measurements (e.g., use of a Marinelli beaker; shielding of the detector; drying, crushing, grinding, mixing of rock; other relevant information): **Before the measurements, the rock sample**

**was dried, crushed, ground, mixed and placed in a Marinelli container (Fig. 24b,c, *Fig. 25*), which was then sealed and left for one month to achieve secular equilibrium in the thorium and uranium series. The grains diameter after crushing the rock sample were less than 1 mm. Measurements were made in a shielded cover made of lead and copper.**

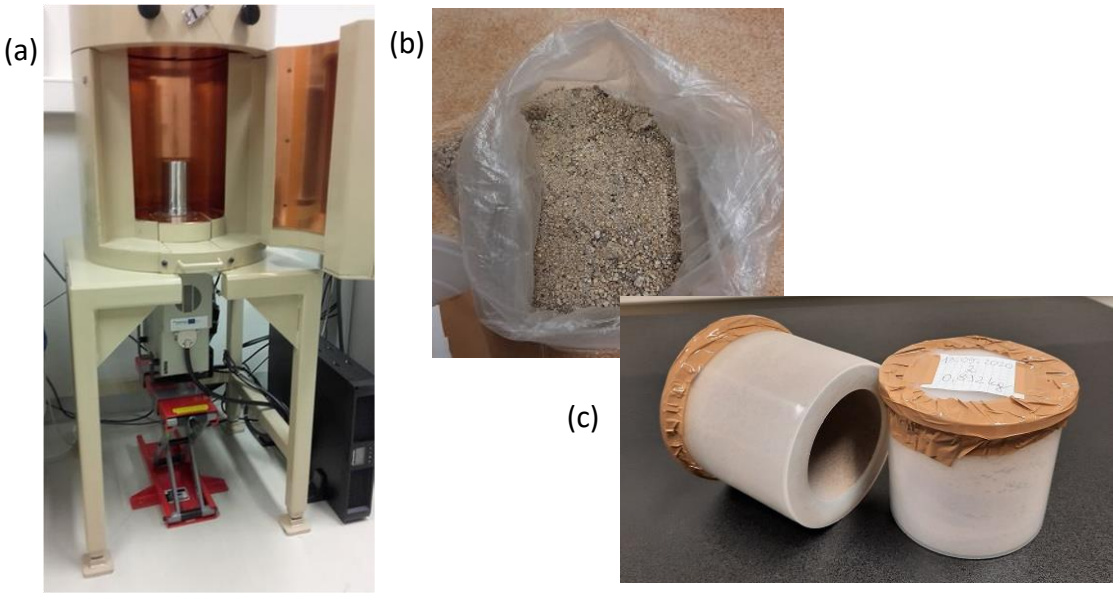


Fig. 24 (a) HPGe detector with shielding, (b) crushed rock sample no. 11, (c) rock sample in Marinelli containers.

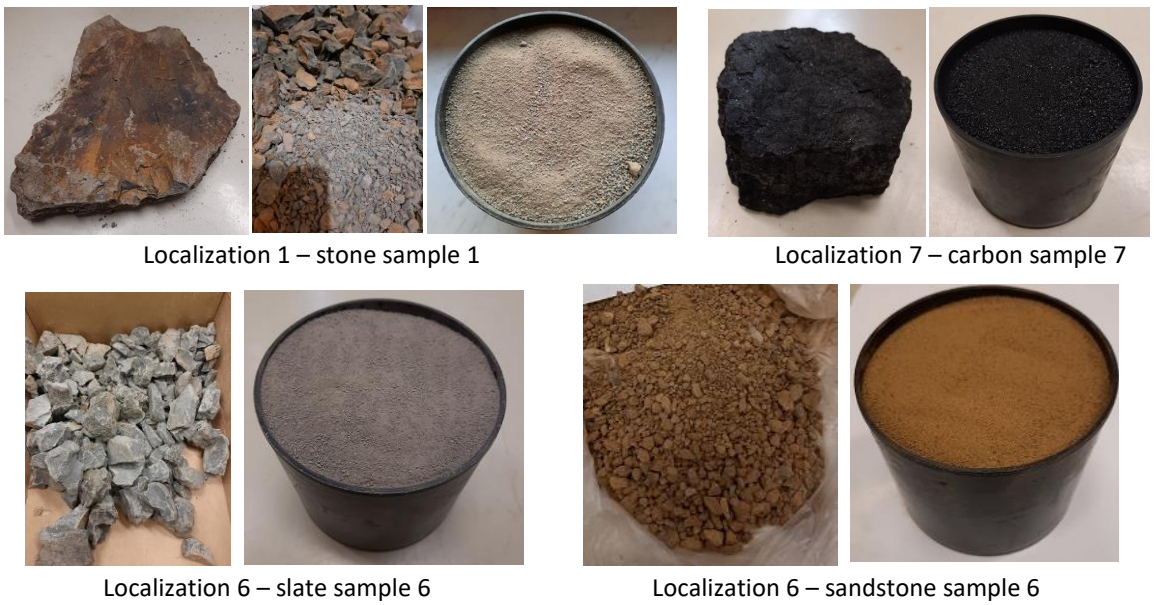


Fig. 25 Stone sample from localization 1, carbon sample from localization 7, slate and sandstone sample from localization 6.

Tab. 11 Results of radium and potassium concentration in rock, stone, slate, sandstone and carbon samples.

| Hall ID (name of sample) | Measu-rement method | Equipment type | Detection relative efficiency [%] | Collection period | Average results [Bq/kg] | | |
|---|---|---|---|---|---|---|---|
| | | | | | $^{226}$Ra | $^{228}$Ra | $^{40}$K |
| Rock sample 1 | Gamma spectro-metry | HPGe detector | 20 | 3.0 days | 9.7±0.4* | 9.4±0.3* | 476±8* |
| Rock sample 2 | | | | 2.8 days | 24.6±0.8* | 25.8±0.5* | 515±8* |
| Rock sample 3 | | | | 2.9 days | 12.3±0.4* | 10.6±0.3* | 453±7* |
| Rock sample 4 | | | | 1.9 days | 14.5±0.5* | 12.6±0.4* | 560±10* |
| Rock sample 5 | | | | 2.1 days | 12.9±0.5* | 12.8±0.3* | 463±8* |
| Rock sample 6 | | | | 4 days | 10.4±0.4* | 11.1±0.3* | 545±9* |
| Rock sample 7 | | | | 2 days | 22.6±0.8* | 17.3±0.4* | 560±10* |
| Rock sample 8 | | | | 2.1 days | 9.7±0.4* | 11.0±0.4* | 466±8* |
| Rock sample 9 | | | | 3 days | 14.2±0.8* | 11.5±0.3* | 535±9* |
| Rock sample 10 | | | | 2.1 days | 10.4±0.4* | 8.4±0.3* | 434±7* |
| Rock sample 11 | | | | 2.7 days | 53.7±1.8* | 31.5±0.7* | 601±10* |
| Rock sample 12 | | | | 3.1 days | 14.7±0.5* | 14.0±0.6* | 557±9* |
| Rock sample 13 | | | | 2 days | 25.8±0.9* | 28.4±0.6* | 485±8* |
| Rock sample 14 | | | | 2.3 days | 35.5±1.2* | 31.5±0.7* | 609±10* |
| Rock sample 15 | | | | 2 days | 24.3±0.9* | 14.8±0.4* | 541±9* |
| Rock sample 16 | | | | 3.9 days | 11.8±0.4* | 12.3±0.3* | 533±8* |
| Rock sample 17 | | | | 1.9 days | 8.1±0.3* | 7.0±0.3* | 521±9* |
| Rock sample 18 | | | | 2.1 days | 11.0±0.4* | 10.4±0.3* | 446±8* |
| Stone sample loc.1 | | | | 2.1 days | 64.9±2.4 | 58.2±1.2 | 685.5±11.2 |
| Stone sample loc.2 | | | | 2.0 days | 53.3±2.0 | 47.2±1.0 | 813.7±13.0 |
| Carbon sample loc.2 | | | | 4.6 days | 3.0±0.1 | 1.2±0.1 | 3.6±0.1 |
| Slate sample loc.6 | | | | 2.1 days | 61.3±2.3 | 51.6±1.0 | 856.6±13.6 |
| Sandstone sample loc.6 | | | | 2.2 days | 26.2±1.0 | 23.8±0.5 | 668.0±10.8 |
| Carbon sample loc.7 | | | | 4.0 days | 4.3±0.2 | 1.8±0.1 | 8.8±0.5 |

*data are presented in A. Walencik-Łata, et al., Characteristics of Natural Background Radiation in the GIG Experimental Mine 'Barbara', Poland. Energies 2022, 15, 685

Gamma-ray spectra:

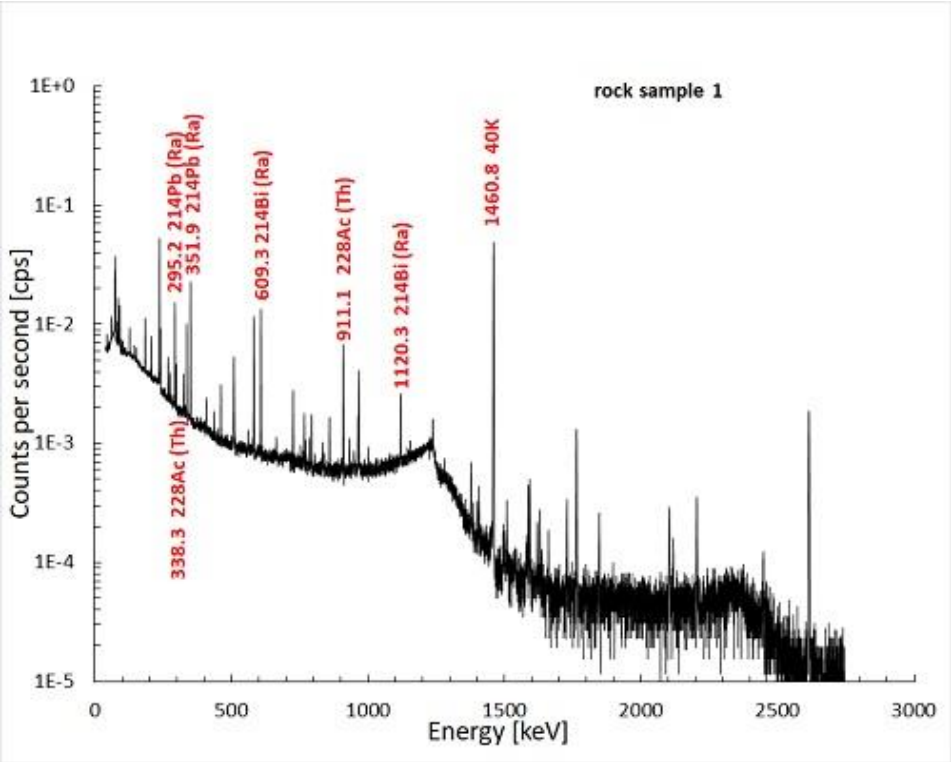


Fig. 26 Gamma-ray spectrum of a rock sample 1.

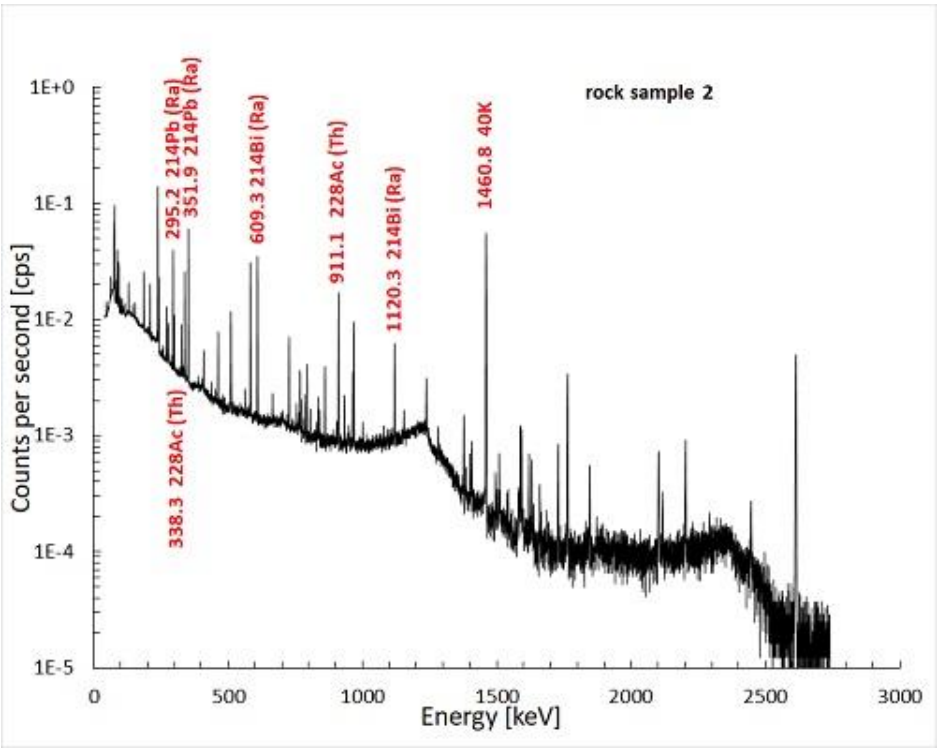


Fig. 27 Gamma-ray spectrum of a rock sample 2.

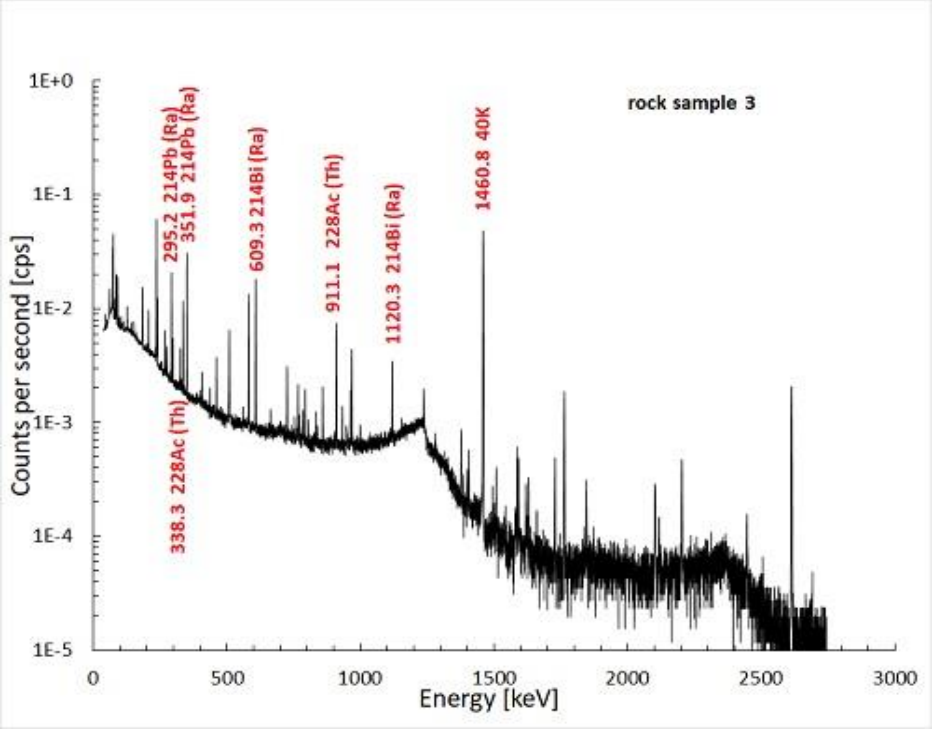


Fig. 28 Gamma-ray spectrum of a rock sample 3.

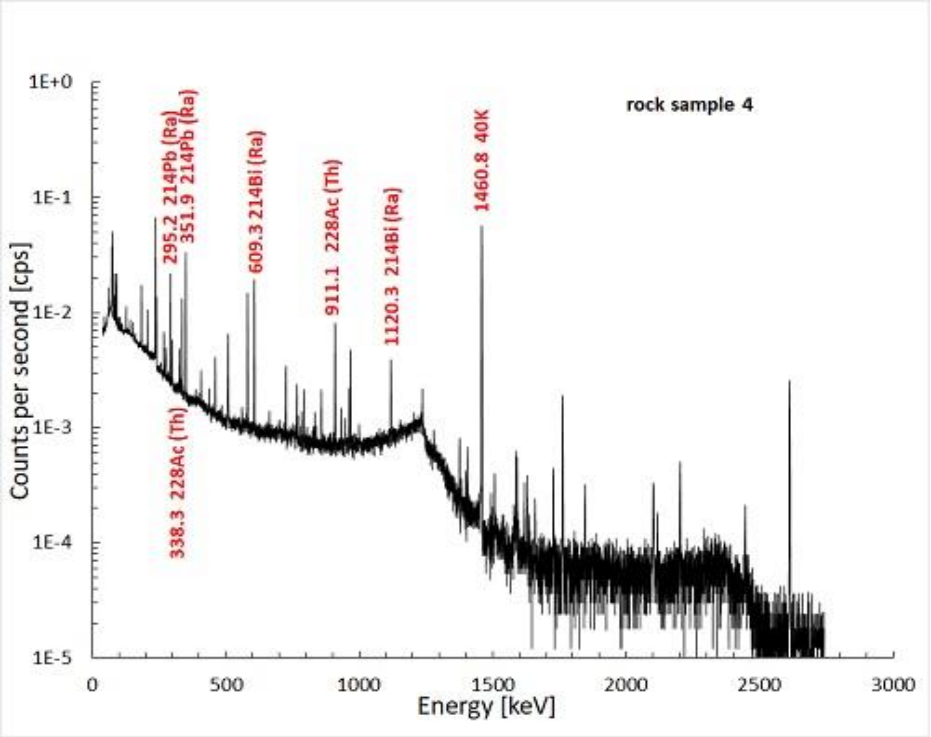


Fig. 29 Gamma-ray spectrum of a rock sample 4.

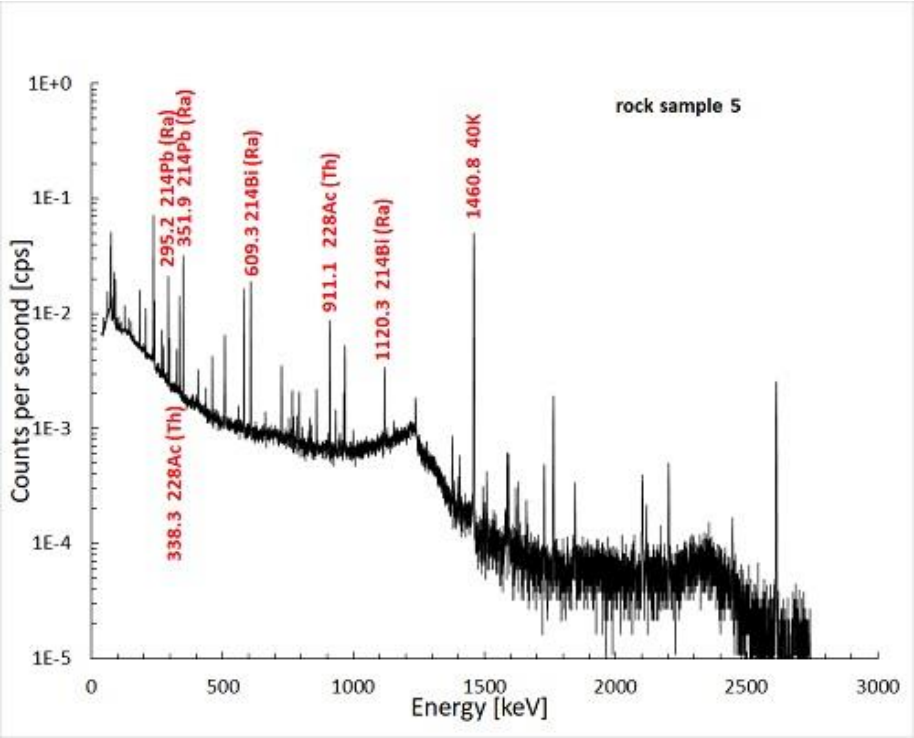


Fig. 30 Gamma-ray spectrum of a rock sample 5.

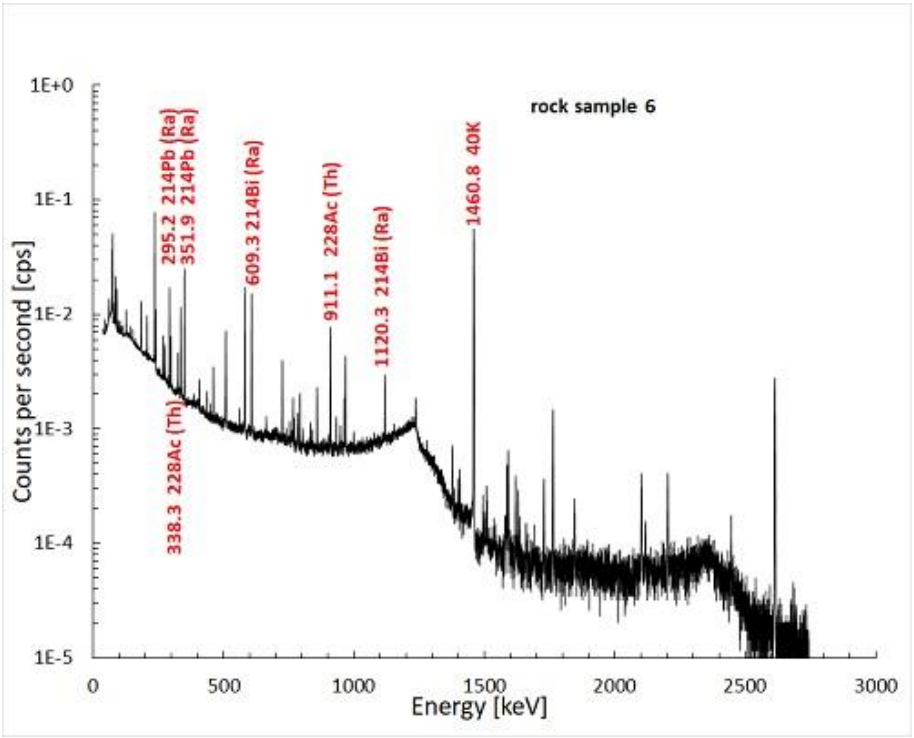


Fig. 31 Gamma-ray spectrum of a rock sample 6.

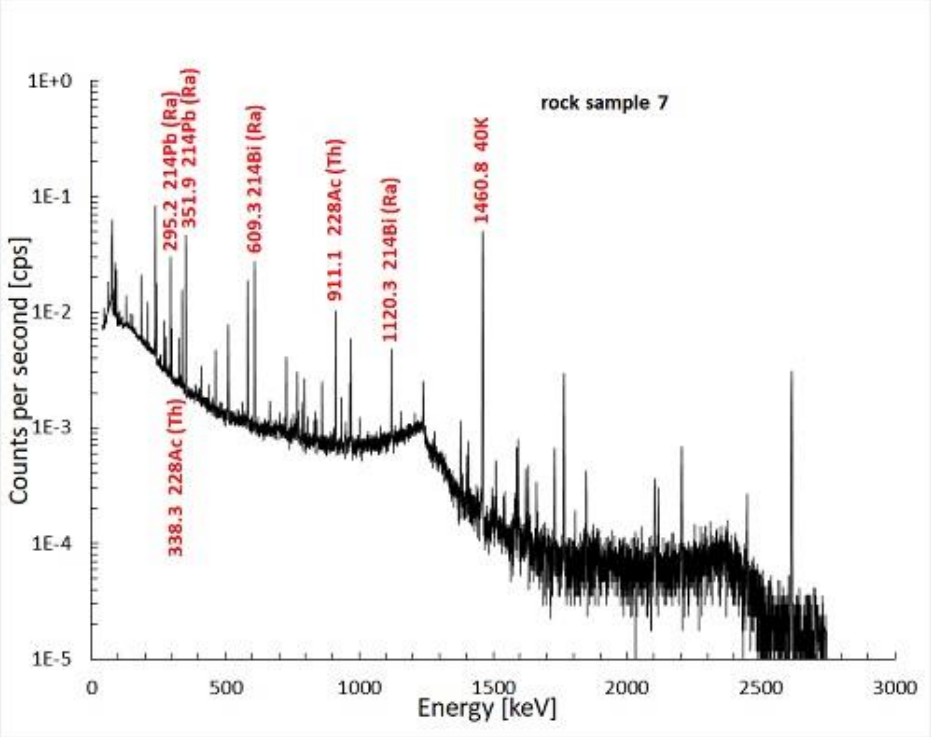


Fig. 32 Gamma-ray spectrum of a rock sample 7.

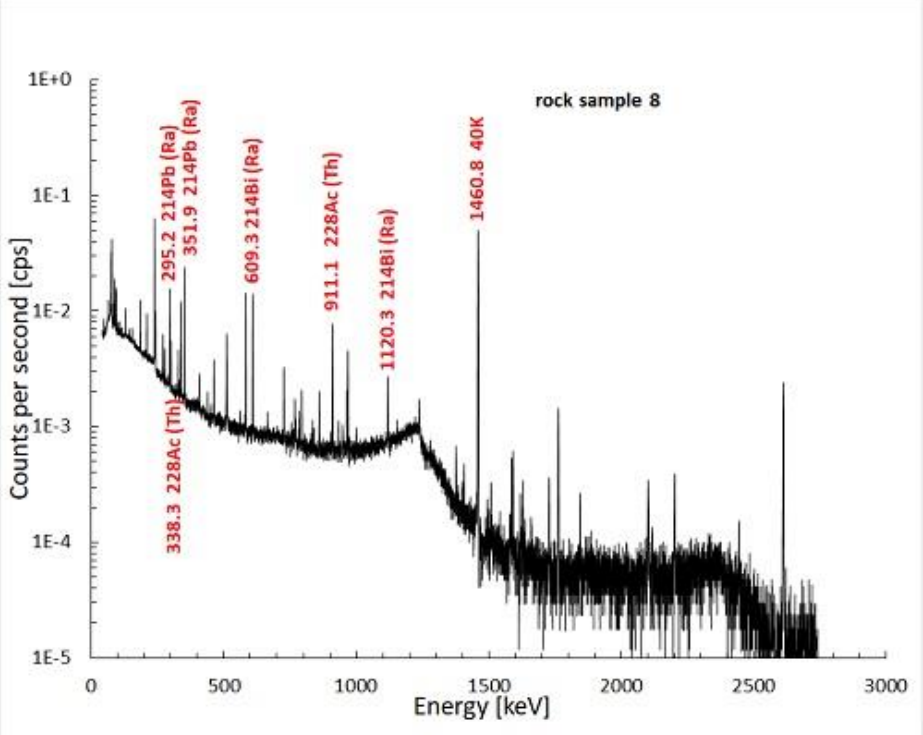


Fig. 33 Gamma-ray spectrum of a rock sample 8.

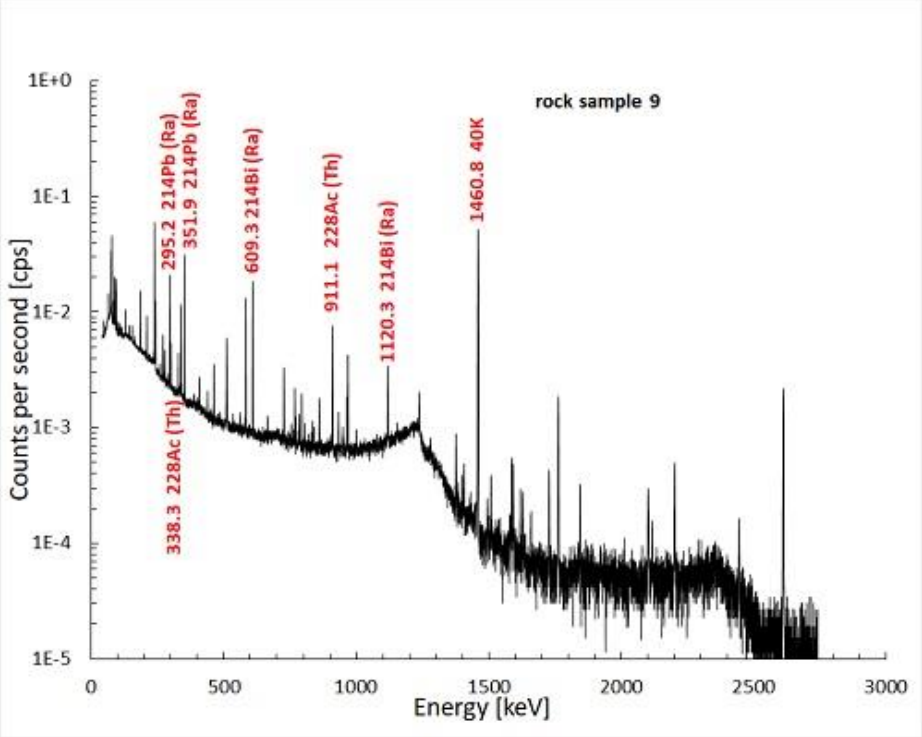


Fig. 34 Gamma-ray spectrum of a rock sample 9.

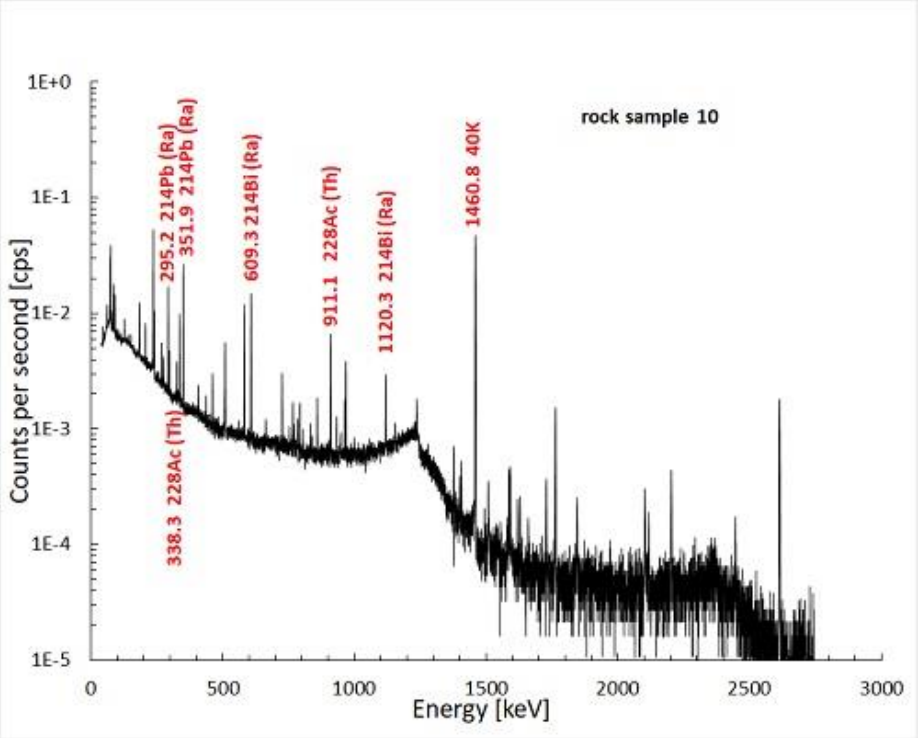


Fig. 35 Gamma-ray spectrum of a rock sample 10.

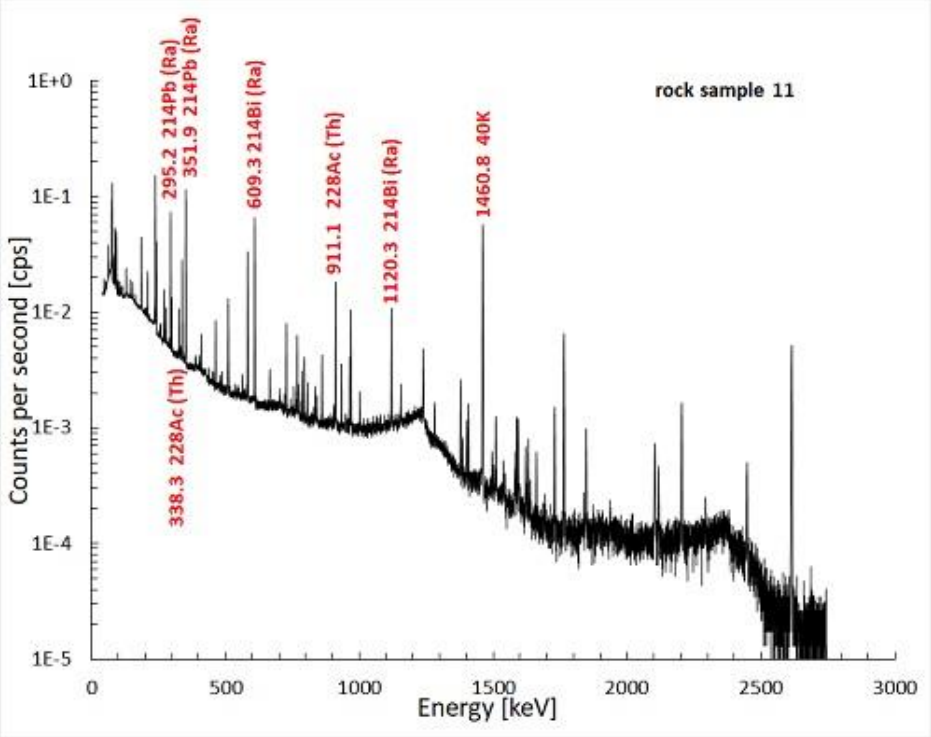


Fig. 36 Gamma-ray spectrum of a rock sample 11.

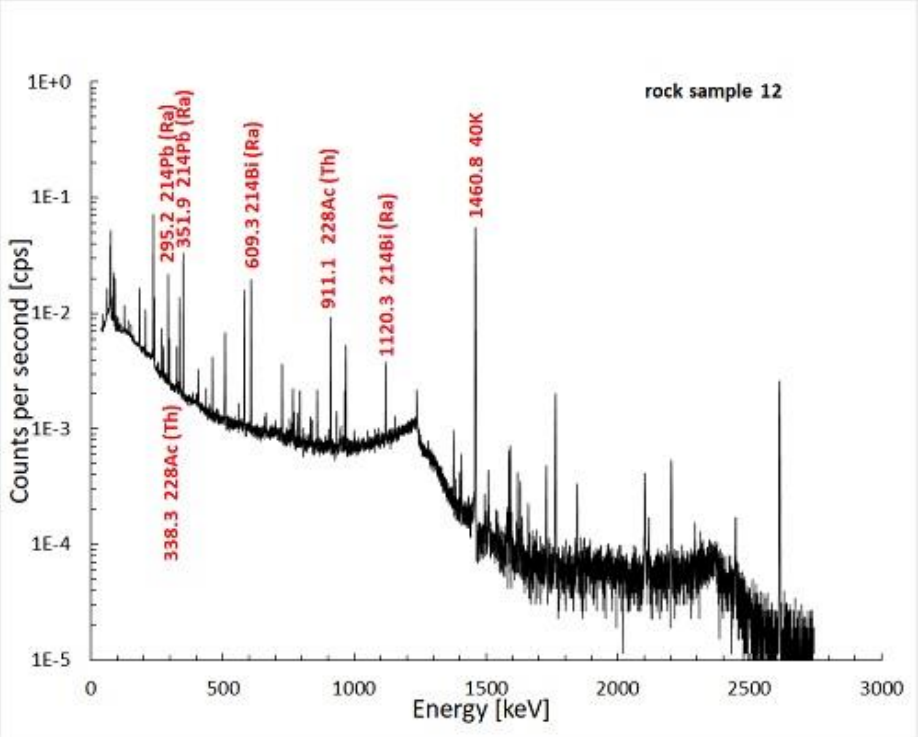


Fig. 37 Gamma-ray spectrum of a rock sample 12.

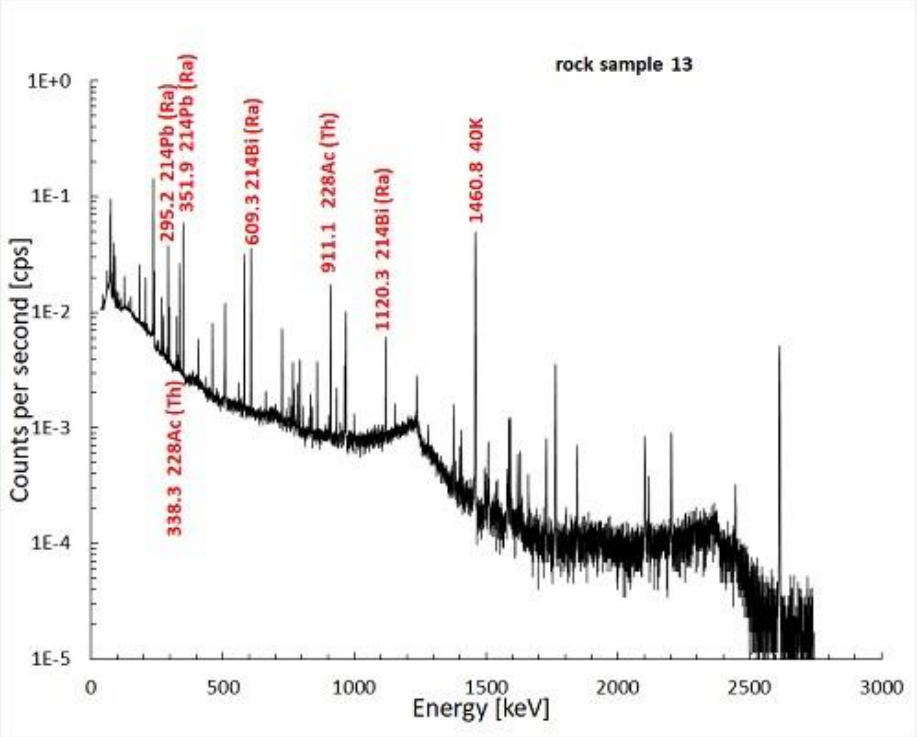


Fig. 38 Gamma-ray spectrum of a rock sample 13.

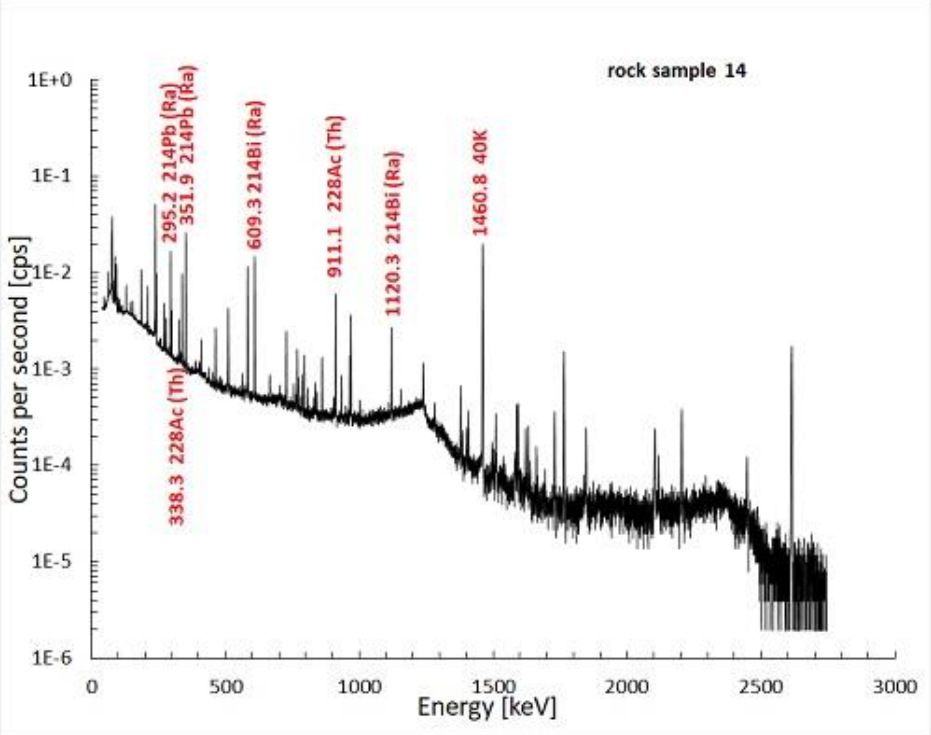


Fig. 39 Gamma-ray spectrum of a rock sample 14.

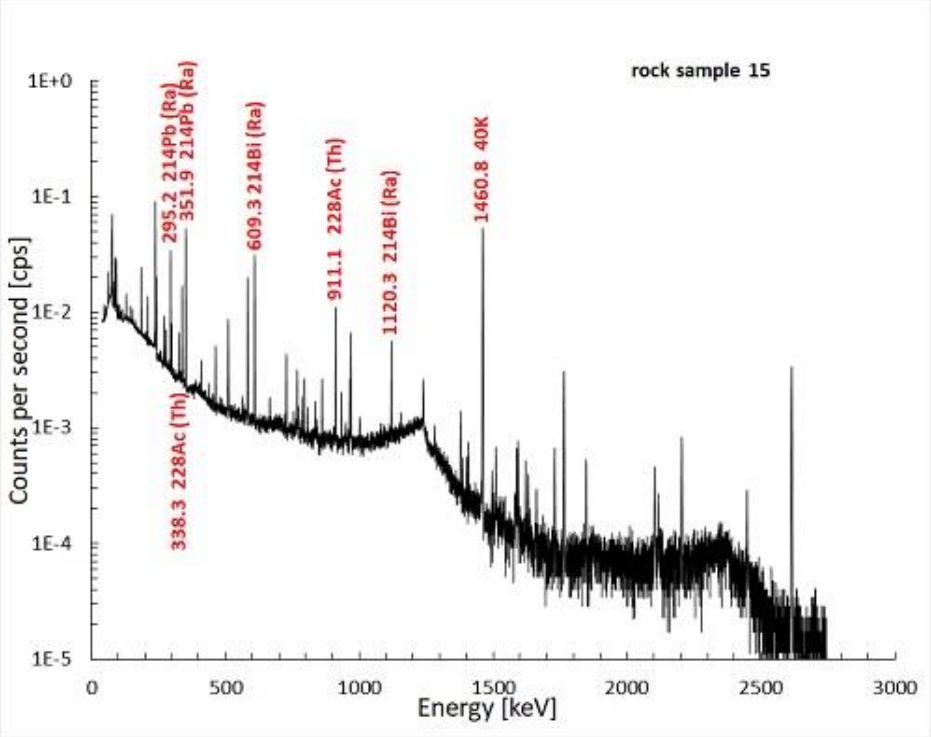


Fig. 40 Gamma-ray spectrum of a rock sample 15.

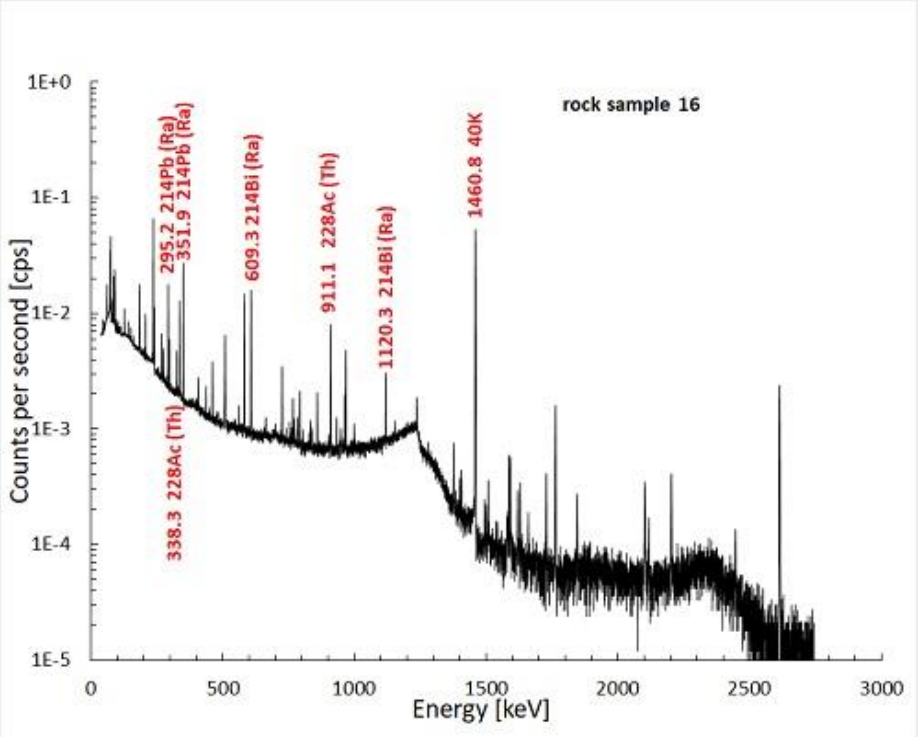


Fig. 41 Gamma-ray spectrum of a rock sample 16.

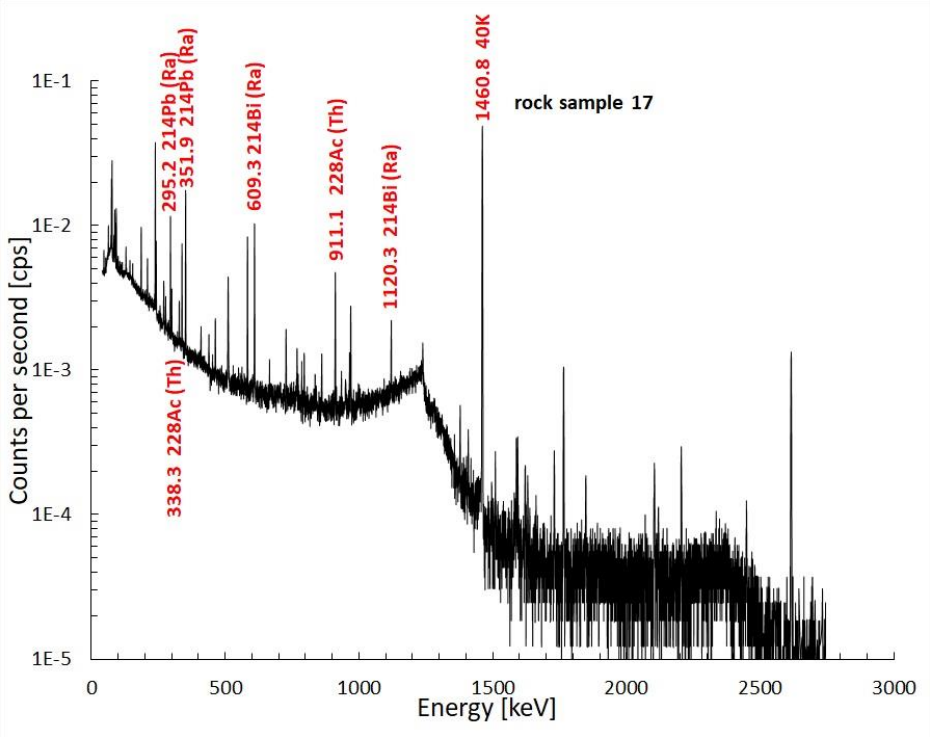


Fig. 42 Gamma-ray spectrum of a rock sample 17.

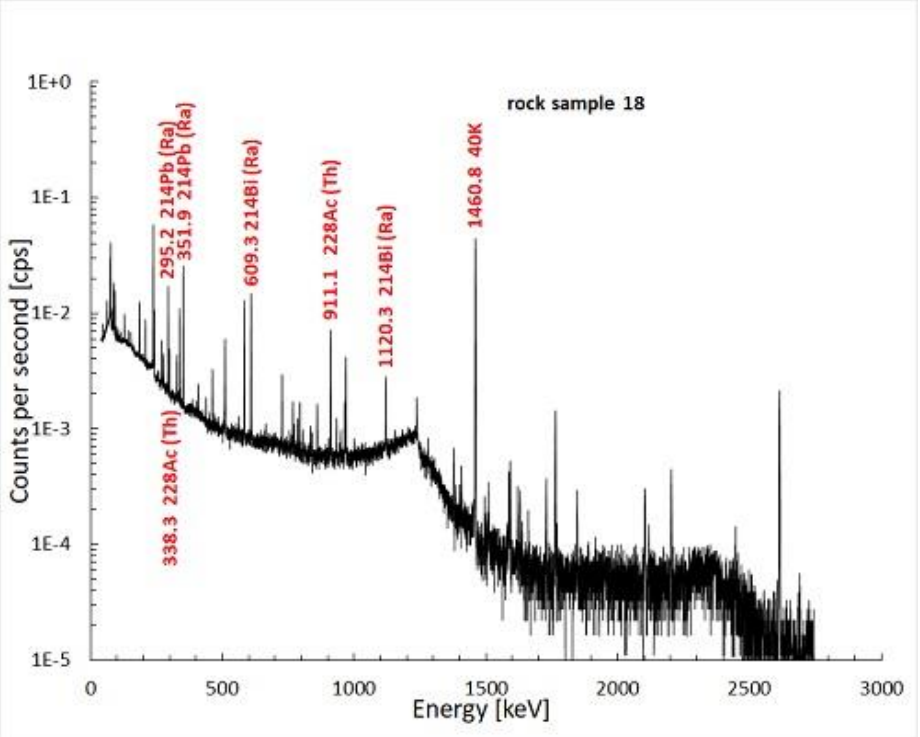


Fig. 43 Gamma-ray spectrum of a rock sample 18.

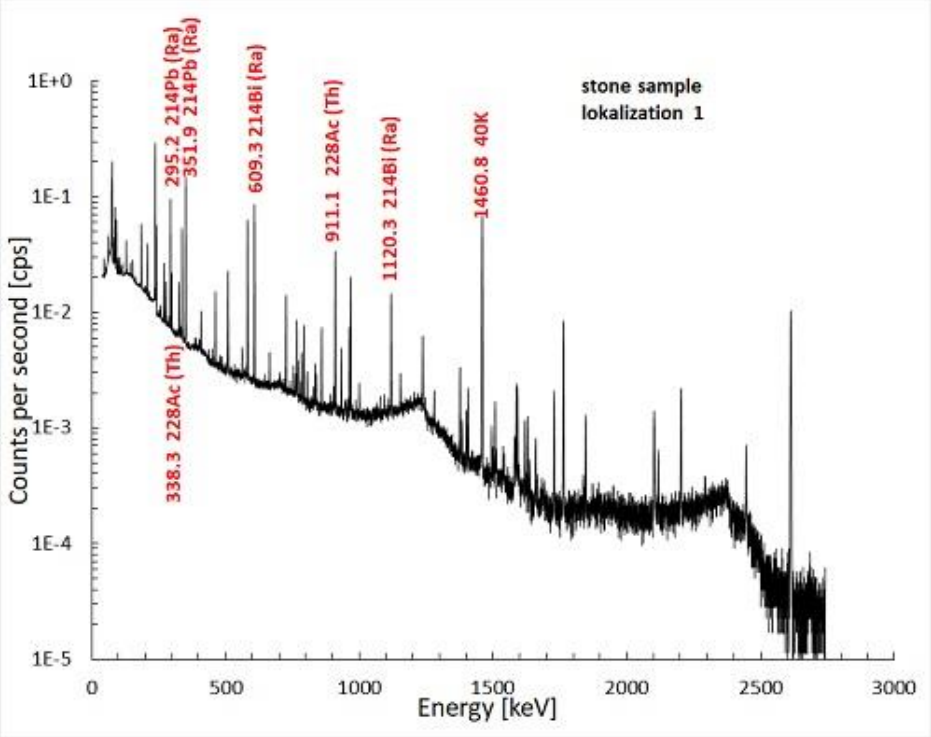


Fig. 44 Gamma-ray spectrum of a stone sample loc.1.

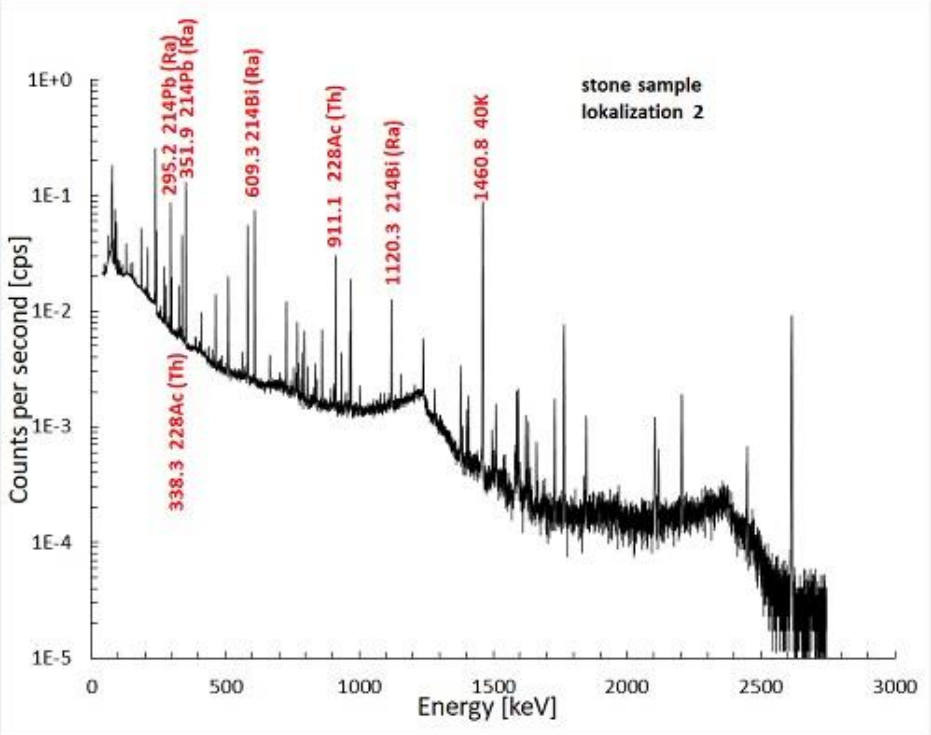


Fig. 45 Gamma-ray spectrum of a stone sample loc.2.

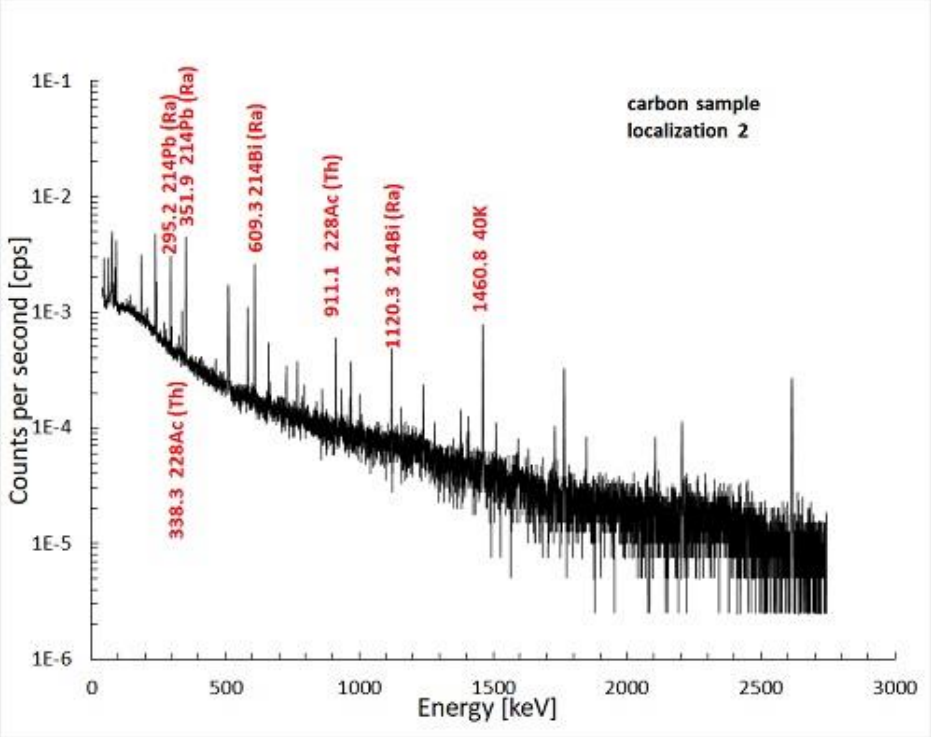


Fig. 46 Gamma-ray spectrum of a carbon sample loc.2.

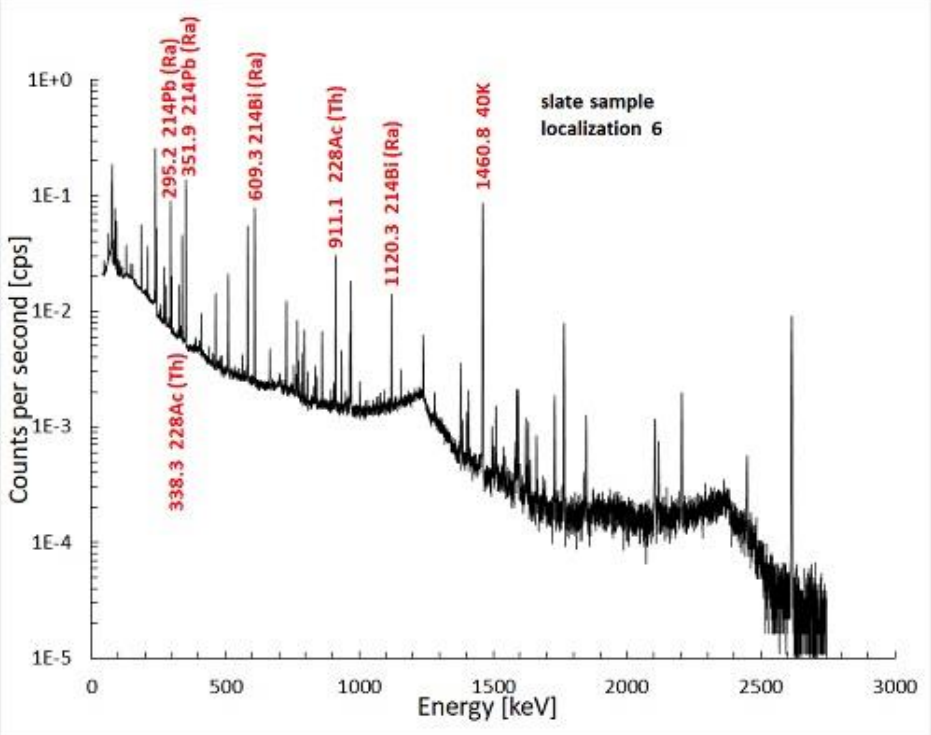


Fig. 47 Gamma-ray spectrum of a slate sample loc.6.

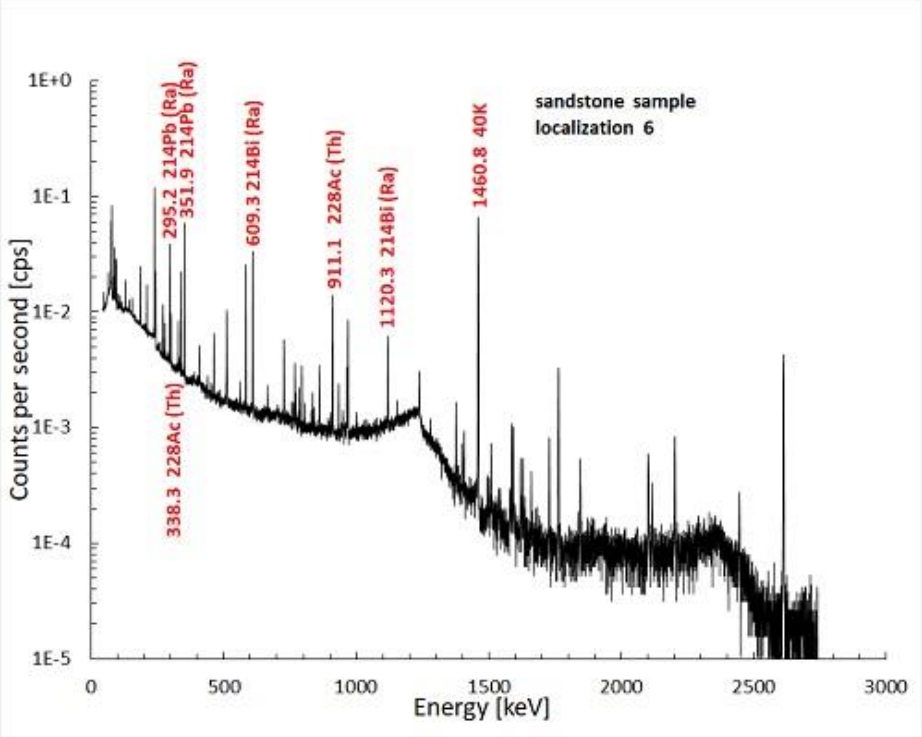


Fig. 48 Gamma-ray spectrum of a sandstone sample loc.6.

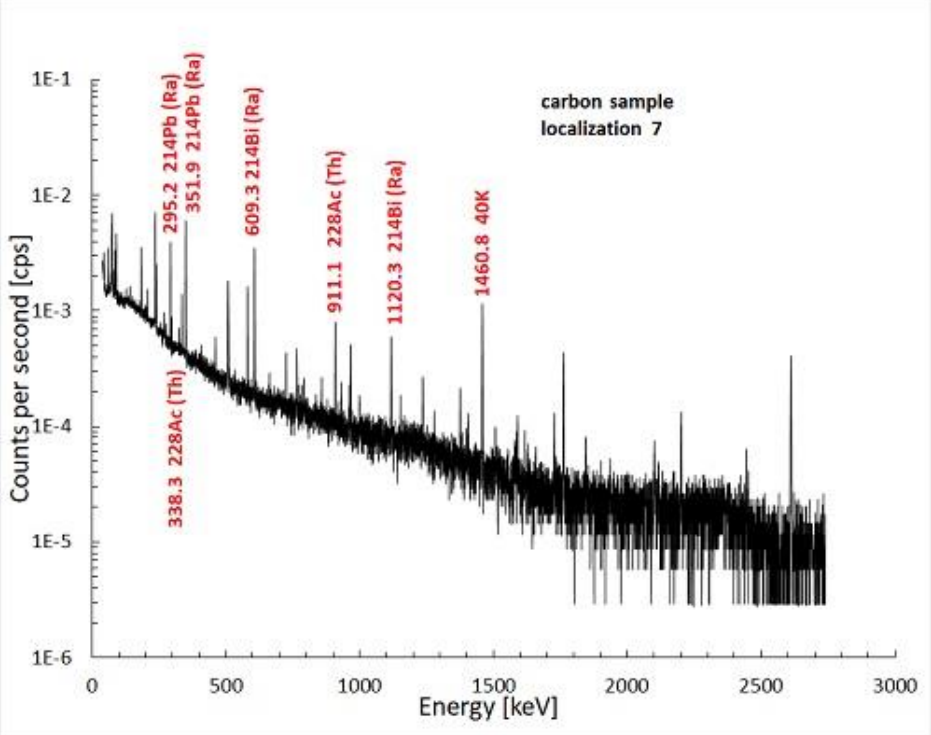


Fig. 49 Gamma-ray spectrum of a carbon sample loc.7.

### *b. Uranium concentration in rock samples*

- Description of the performed chemical procedure

The concentration of uranium $^{234}U$ and $^{238}U$ isotopes in the rock samples were determined by semiconductor alpha spectrometry and 7401VR (Canberra, USA) and Alpha Analyst™ (Mirion Technologies (Canberra), Inc., USA) spectrometers (***Fig. 50*a,b**). A radiochemical procedure was applied to prepare an alpha spectrometric source before measurement. For this purpose, wet mineralization of the rock sample was performed using hot acids: HF, $HNO_3$, HCl, with $H_3BO_3$. Uranium was pre-concentrated with iron and co-precipitated at pH 9. The separation of U was performed using the anion exchange resin Dowex 1×8 ($Cl^-$ type, 200-400 mesh) based on a procedure worked out by Suomela (1993). The spectrometric source was prepared by co-precipitation of U with $NdF_3$ and deposition on polypropylene disks (0.1 µm) (Pall Corporation).

References:

J. Suomela, Method for determination of U-isotopes in water, Swedish Radiation Institute, Stockholm, SSI-rapport, 0282-4434, 93:14 (1993).

(a) 


(b) 


**Fig. 50 (a) The alpha spectrometer 7401VR (Canberra, USA), (b) The alpha spectrometer Alpha Analyst™ (Mirion Technologies (Canberra), Inc., USA).**

- Information about measurement and results

Tab. 12 Results of uranium radioisotopes concentration in rock samples.

| Hall ID (name of sample) | Measu-rement method | Equipment type | Collection period | Limit of detection | Average results [Bq/kg] | | ratio $^{234}U/^{238}U$ | U [ppm] |
|---|---|---|---|---|---|---|---|---|
| | | | | | $^{234}U$ | $^{238}U$ | | |
| Rock sample 1 | Alpha spectro-scopy | spectrometers 7401VR (Canberra–Packard) and Alpha Analyst™ (Mirion Technologies (Canberra), Inc., USA) | 1-7 days | 0.5 mBq/l for both $^{234,238}U$ isotopes and 0.5 l initial sample volume | 10.4±0.8* | 10.4±0.8* | 1.00±0.10* | 0.84±0.06 |
| Rock sample 2 | | | | | 22.2±1.1* | 21.6±1.0* | 1.03±0.07* | 1.75±0.08 |
| Rock sample 3 | | | | | 14.9±1.2* | 14.7±1.1* | 1.01±0.11* | 1.19±0.09 |
| Rock sample 4 | | | | | 15.3±1.1* | 15.2±1.0* | 1.01±0.10* | 1.23±0.08 |
| Rock sample 5 | | | | | 15.8±1.0* | 15.9±1.0* | 0.99±0.09* | 1.29±0.08 |
| Rock sample 6 | | | | | 11.9±1.0* | 10.7±0.9* | 1.11±0.13* | 0.87±0.07 |

*data are presented in A. Walencik-Łata, et al., Characteristics of Natural Background Radiation in the GIG Experimental Mine 'Barbara', Poland. Energies 2022, 15, 685

Alpha spectra:

EM 'Barbara' mine – rock sample 1 Time of measurement: 43 h

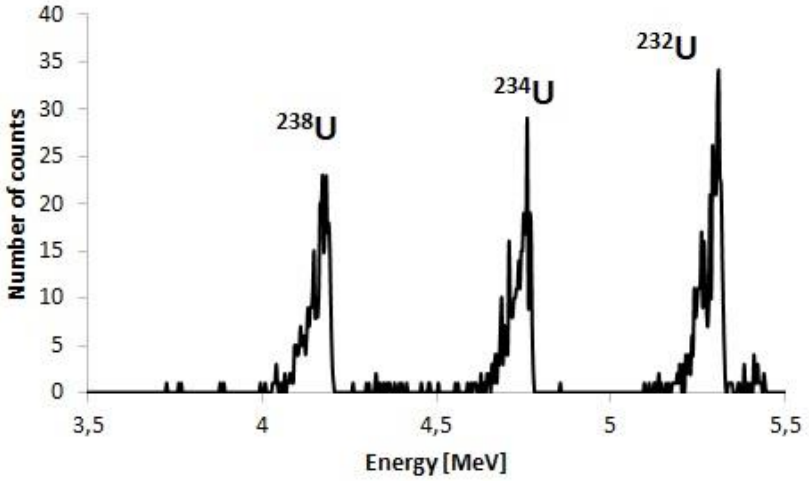


Fig. 51 The alpha spectrum of a rock sample 1 – EM 'Barbara'.

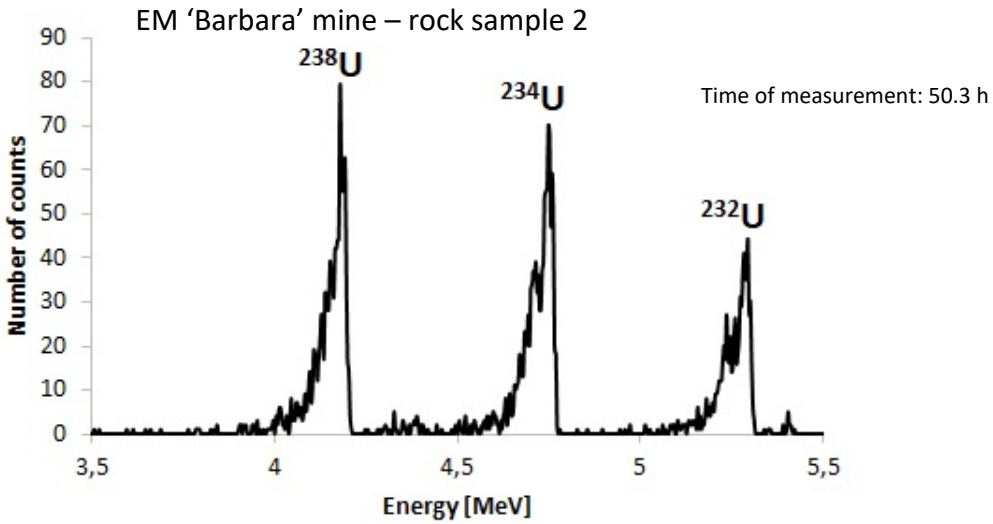


Fig. 52 The alpha spectrum of a rock sample 2 – EM 'Barbara'.

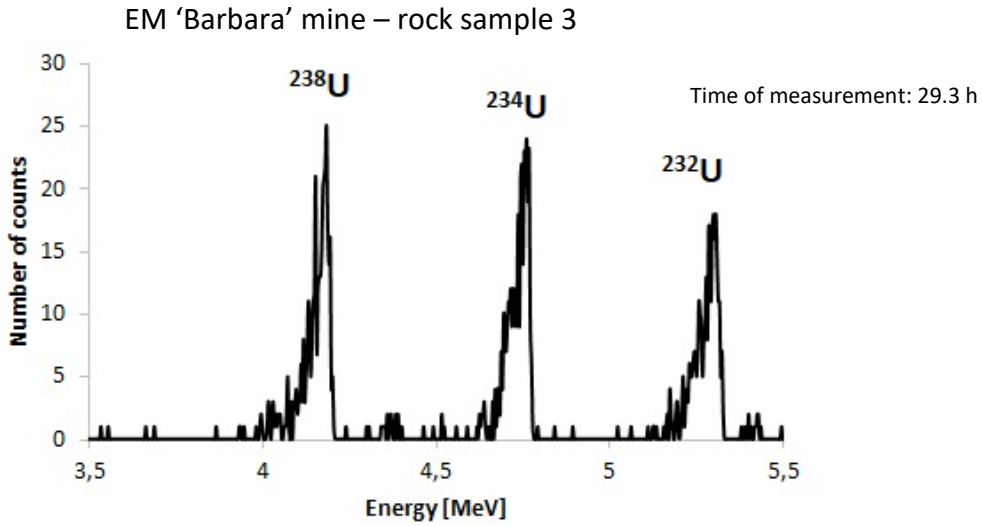


Fig. 53 The alpha spectrum of a rock sample 3 – EM 'Barbara'.

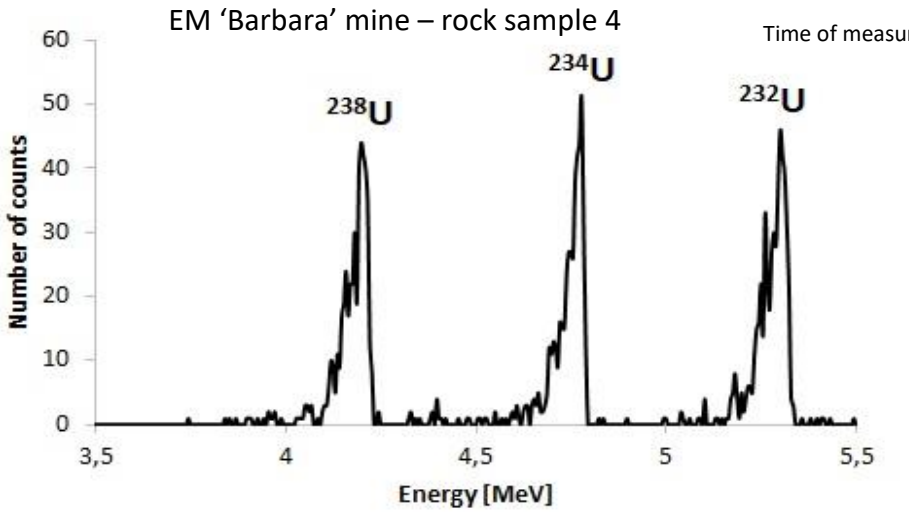


Fig. 54 The alpha spectrum of a rock sample 4 – EM 'Barbara'.

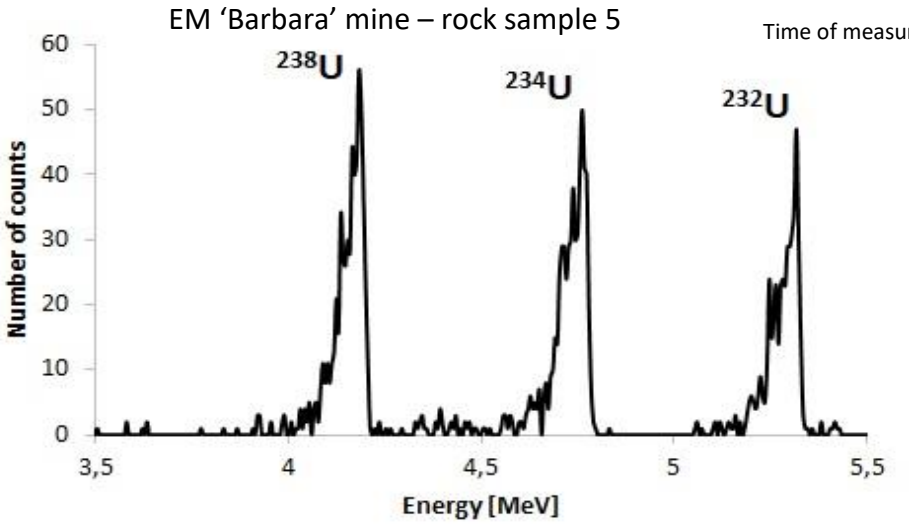


Fig. 55 The alpha spectrum of a rock sample 5 – EM 'Barbara'.

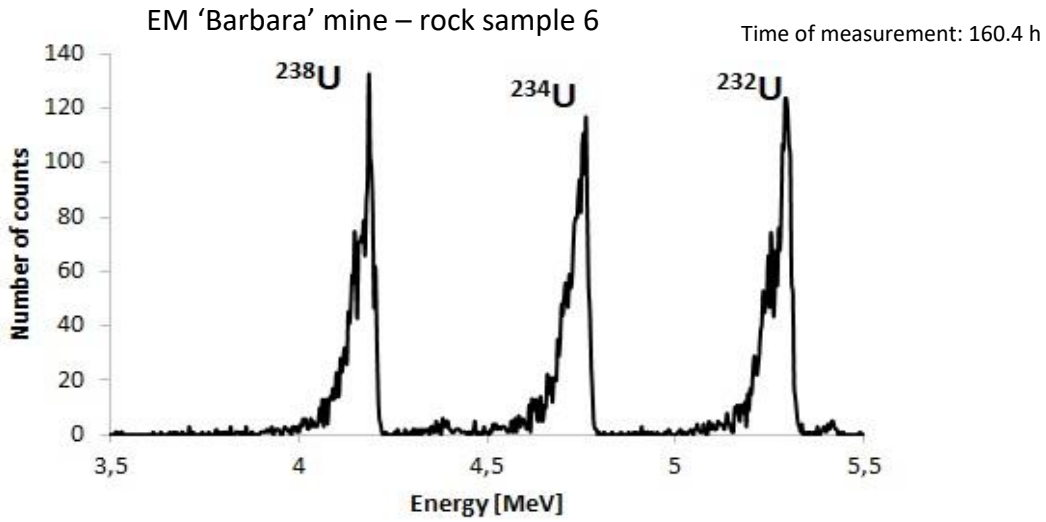


Fig. 56 The alpha spectrum of a rock sample 6 – EM 'Barbara'.

### *c. Neutron activation of the rock sample*

- Information about measurement and results

Before the measurements, the rock samples were dried, crushed, and mixed. The grain diameter of the crushed rock sample was less than 1 mm. Then the sample was placed in a plastic bag and activated by neutron flux from a $^{252}$Cf source (***Fig. 57*b**) by period of one month. Immediately after activation, the gamma-ray spectrum was measured by gamma spectroscopy with a lead-shielded HPGe detector (***Fig. 57*a**). Measurements were carried out in several cycles, in short cycles to determine the short-lived isotopes produced during the activation of the sample by neutrons, and in long cycles to determine the long-lived isotopes.

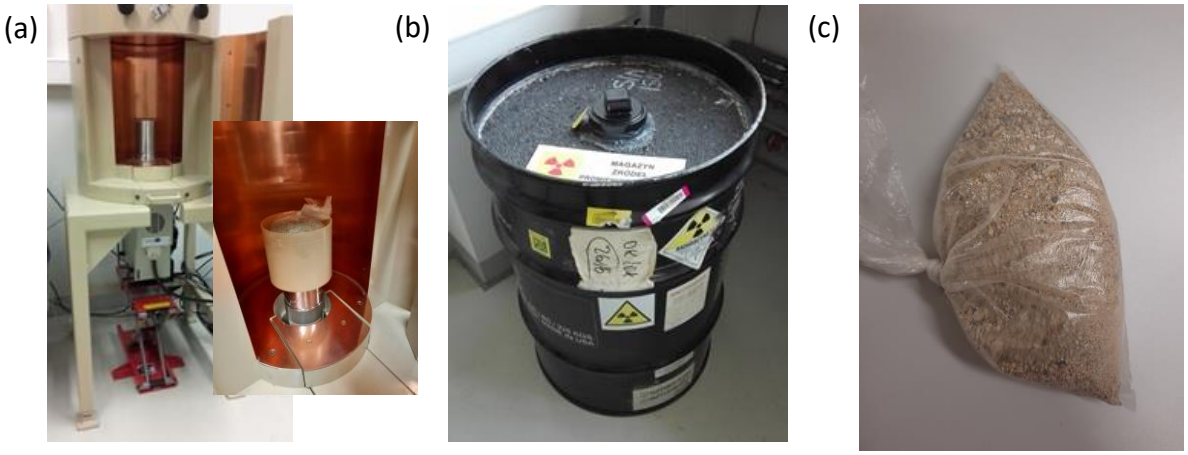


Fig. 57 (a) HPGe detector, (b) source ($^{252}$Cf) of neutron activation, (c) rock sample after neutron activation for gamma-ray spectrometry.

- Information about measurement and results

Tab. 13 Neutron activation results of the rock sample from EM 'Barbara'*.

| Hall ID (name of sample) | Measure-ment method | Equipment type | Detection relative efficiency [%] | Collection period | Source of neutron activation | Neutron flux of the source | Activated isotopes |
|---|---|---|---|---|---|---|---|
| Sample 11 | Gamma scpectrometry | HPGe detector | 20 | Short measurements and long measurements by a few days | californium ($^{252}$Cf) | $10^5$ n/cm$^2$/s | $^{57}$Ni, $^{46}$Sc, $^{56}$Mn, $^{24}$Na, $^{42}$K, $^{140}$La |

*data are presented in A. Walencik-Łata, et al., Characteristics of Natural Background Radiation in the GIG Experimental Mine 'Barbara', Poland. Energies 2022, 15, 685

Analysis of rock sample, which underwent neutron activation.

Tab. 14 Comparison of counts per second for a rock sample before and after neutron activation of a rock sample.

| Isotope | Energy [keV] | Counts per second | | |
|---|---|---|---|---|
| | | Rock sample before neutron activation | Rock sample 67 h after neutron activation | Rock sample 101.7 h after neutron activation |
| $^{210}$Pb | 46.5 | 0.01400 | 0.00810 | 0.00810 |
| $^{214}$Pb | 53.2 | 0.00779 | | |
| $^{230}$Th | 63.3 | 0.04613 | 0.02314 | 0.02327 |

| | | | | |
|---|---|---|---|---|
| $^{230}$Th | 67.7 | 0.00236 | 0.00184 | 0.00271 |
| X Pb $K_{\alpha 2}$ | 72.8 | 0.01307 | 0.00658 | 0.00684 |
| X Pb $K_{\alpha 1}$ | 74.97 | 0.19313 | 0.08356 | 0.08316 |
| $^{227}$Th | 77.1 | 0.30181 | 0.13156 | 0.12848 |
| X Po $K_{\alpha 1}$ | 79.3 | 0.00289 | 0.00101 | 0.00173 |
| X Rn $K_{\alpha 2}$ | 81.1 | 0.00278 | 0.00098 | 0.00223 |
| X Rn $K_{\alpha 1}$ | 83.8 | 0.03198 | 0.01360 | 0.01529 |
| X Bi $K_{\beta 1}$ | 87.3 | 0.10002 | 0.04410 | 0.04267 |
| X Bi $K_{\beta 2}$ | 89.8 | 0.05874 | 0.02391 | 0.02441 |
| $^{234}$Th | 92.7 | 0.10448 | 0.05135 | 0.05070 |
| X U $K_{\alpha 1}$ | 98.4 | 0.00711 | | |
| $^{228}$Ac | 99.5 | 0.01388 | 0.00777 | 0.00931 |
| X Ra $K_{\beta 1}$ | 103 | | 0.00981 | 0.00396 |
| X Th $K_{\beta 1}$ | 105.6 | 0.01692 | 0.00896 | 0.00728 |
| X Th $K_{\beta 2}$ | 108.6 | 0.00729 | | 0.00267 |
| $^{234}$Th | 112.8 | 0.00508 | 0.00369 | 0.00155 |
| $^{212}$Pb | 115.2 | 0.00656 | 0.00304 | 0.00244 |
| $^{228}$Ac | 129.1 | 0.02296 | 0.01127 | 0.01029 |
| $^{228}$Th | 131.3 | | | 0.00116 |
| $^{235}$U | 143.8 | 0.01039 | 0.00423 | 0.00601 |
| $^{228}$Ac | 154 | 0.01328 | 0.00640 | 0.00594 |
| $^{235}$U | 163.4 | 0.00506 | 0.00206 | 0.00367 |
| $^{235}$U | 186.1 | 0.12164 | 0.05612 | 0.05247 |
| $^{228}$Ac | 191.6 | 0.00196 | | |
| $^{228}$Ac | 199.4 | 0.00315 | | |
| $^{235}$U | 205.3 | 0.00561 | 0.00199 | 0.00184 |
| $^{228}$Ac | 209.3 | 0.03812 | 0.01733 | 0.01541 |
| $^{228}$Th | 216.5 | 0.00277 | | 0.00211 |
| $^{227}$Th | 236 | 0.00853 | 0.00349 | 0.00294 |
| $^{212}$Pb | 238.6 | 0.43551 | 0.18229 | 0.17541 |
| $^{214}$Pb | 242 | 0.11534 | 0.04953 | 0.04710 |
| $^{208}$Tl | 252.6 | 0.00179 | 0.00102 | 0.00100 |
| $^{227}$Th | 256.2 | 0.00487 | 0.00239 | 0.00162 |
| $^{214}$Pb/$^{227}$Ra | 258.9 | 0.00774 | 0.00452 | 0.00286 |
| $^{228}$Ac | 270.2 | 0.04244 | 0.01631 | 0.01759 |
| $^{214}$Pb | 274.8 | 0.00320 | 0.00193 | 0.00090 |
| $^{208}$Tl/$^{227}$Ra | 277.4 | 0.01666 | 0.00858 | 0.00657 |
| $^{212}$Bi | 288.1 | 0.00193 | | 0.00057 |
| $^{214}$Pb | 295.2 | 0.21707 | 0.08974 | 0.08805 |
| $^{212}$Pb/$^{227}$Ra | 300.1 | 0.02595 | 0.00983 | 0.00995 |
| $^{227}$Ra | 302.7 | 0.00117 | | |

| | | | | |
|---|---|---|---|---|
| $^{214}$Pb | 323.8 | 0.00036 | | 0.00064 |
| $^{228}$Ac | 327.6 | 0.02033 | 0.00889 | 0.00801 |
| $^{228}$Ac | 332.4 | 0.00193 | | |
| $^{228}$Ac | 338.3 | 0.08217 | 0.03191 | 0.03145 |
| $^{228}$Ac | 341 | 0.00226 | | |
| $^{214}$Pb | 351.9 | 0.36334 | 0.15232 | 0.14524 |
| $^{214}$Bi | 386.8 | 0.00237 | | 0.00108 |
| $^{214}$Bi | 388.9 | 0.00351 | | 0.00134 |
| $^{219}$Rn | 401.8 | 0.00343 | 0.00006 | 0.00137 |
| $^{214}$Bi | 405.7 | | | 0.00121 |
| $^{228}$Ac | 409.5 | 0.01009 | 0.00424 | 0.00444 |
| $^{214}$Bi | 426.5 | 0.00160 | | |
| $^{40}$K (DEP) | 438.8 | 0.00397 | 0.00153 | 0.00164 |
| $^{212}$Bi | 452.8 | 0.00189 | | |
| $^{214}$Bi | 454.8 | 0.00165 | | |
| $^{228}$Ac | 463 | 0.02421 | 0.00968 | 0.00918 |
| $^{214}$Bi | 474.4 | | | 0.00008 |
| $^{214}$Pb | 480.4 | 0.00139 | | 0.00094 |
| $^{214}$Pb/$^{140}$La | 487.1 | 0.00410 | 0.00183 | 0.00125 |
| $^{228}$Ac | 503.8 | 0.00001 | | |
| $^{208}$Tl | 510.8 | 0.04917 | 0.02644 | 0.02596 |
| $^{228}$Ac | 546.5 | 0.00049 | | 0.00053 |
| $^{228}$Ac | 562.5 | 0.00454 | 0.00119 | 0.00097 |
| $^{214}$Pb | 580.1 | 0.00245 | | 0.00061 |
| $^{208}$Tl | 583.2 | 0.12447 | 0.04912 | 0.04890 |
| $^{214}$Bi | 609.3 | 0.25491 | 0.10412 | 0.10216 |
| $^{214}$Bi | 665.5 | 0.00643 | 0.00305 | 0.00307 |
| $^{214}$Bi | 703.1 | 0.00282 | 0.00141 | 0.00095 |
| $^{228}$Ac | 707.4 | | 0.00084 | |
| $^{214}$Bi | 719.9 | 0.00110 | | 0.00106 |
| $^{212}$Bi | 727.2 | 0.02645 | 0.01058 | 0.01012 |
| $^{214}$Bi(DEP) | 742.5 | 0.00223 | 0.00038 | |
| $^{228}$Ac | 755.5 | 0.00422 | 0.00070 | 0.00175 |
| $^{208}$Tl | 763.1 | 0.00165 | 0.00042 | 0.00082 |
| $^{214}$Bi | 768.4 | 0.02236 | 0.00907 | 0.00950 |
| $^{228}$Ac | 772.3 | 0.00467 | 0.00154 | 0.00196 |
| $^{228}$Ac | 782.1 | 0.00151 | | |
| $^{212}$Bi/$^{214}$Pb | 785.4 | 0.00911 | 0.00373 | 0.00312 |
| $^{228}$Ac | 795 | 0.01395 | 0.00559 | 0.00536 |
| $^{214}$Bi | 806.2 | 0.00490 | 0.00224 | 0.00198 |
| $^{228}$Ac | 830.5 | 0.00221 | | |

| | | | | |
|---|---|---|---|---|
| $^{228}$Ac | 835.7 | 0.00532 | 0.00245 | 0.00169 |
| $^{214}$Pb | 839 | 0.00513 | 0.00147 | 0.00163 |
| **$^{56}$Mn** | **846.8** | | 0.00031 | |
| $^{208}$Tl | 860.6 | 0.01341 | 0.00595 | 0.00534 |
| **$^{46}$Sc** | **889.3** | | 0.00034 | 0.00051 |
| $^{228}$Ac | 904.2 | 0.00190 | 0.00065 | 0.00080 |
| 228Ac | 911.2 | 0.07908 | 0.03190 | 0.03131 |
| $^{214}$Bi | 934.1 | 0.01140 | 0.00457 | 0.00452 |
| $^{228}$Ac | 964.8 | 0.01533 | 0.00642 | 0.00611 |
| $^{228}$Ac | 969 | 0.04651 | 0.01859 | 0.01828 |
| $^{234m}$Pa | 1001 | 0.00415 | 0.00158 | 0.00218 |
| $^{214}$Bi | 1032.4 | 0.00062 | | |
| $^{214}$Bi | 1052 | 0.00120 | | 0.00017 |
| $^{228}$Ac | 1165.2 | 0.00085 | | |
| $^{214}$Bi | 1070 | 0.00076 | 0.00029 | 0.00034 |
| $^{212}$Bi | 1078.6 | 0.00149 | 0.00012 | 0.00068 |
| $^{228}$Ac | 1110.6 | 0.00114 | | 0.00007 |
| **$^{46}$Sc/$^{214}$Bi** | **1120.2** | 0.05102 | 0.02123 | 0.02036 |
| $^{214}$Bi | 1155.2 | 0.00552 | 0.00211 | 0.00237 |
| $^{214}$Bi | 1207.7 | 0.00113 | 0.00055 | 0.00027 |
| $^{214}$Bi | 1238.1 | 0.01940 | 0.00779 | 0.00736 |
| $^{228}$Ac | 1247.1 | | | 0.00001 |
| $^{214}$Bi | 1281 | 0.00418 | 0.00193 | 0.00137 |
| **$^{24}$Na** | **1368.6** | | 0.00478 | |
| $^{214}$Bi/**$^{57}$Ni** | 1377.7 | 0.01198 | 0.00546 | 0.00517 |
| $^{214}$Bi | 1385.3 | 0.00224 | 0.00076 | 0.00080 |
| $^{214}$Bi | 1401.5 | 0.00382 | 0.00183 | 0.00152 |
| $^{214}$Bi | 1408 | 0.00658 | 0.00283 | 0.00282 |
| $^{40}$K | 1460.8 | 0.32417 | 0.13591 | 0.13247 |
| $^{228}$Ac | 1495.9 | 0.00175 | 0.00074 | 0.00059 |
| $^{228}$Ac | 1501.6 | 0.00074 | 0.00028 | |
| $^{214}$Bi | 1509.2 | 0.00589 | 0.00256 | 0.00181 |
| $^{214}$Bi | 1512.7 | 0.00077 | 0.00032 | 0.00000 |
| **$^{42}$K** | **1524.7** | | 0.00108 | 0.00000 |
| $^{214}$Bi | 1538.5 | 0.00111 | | 0.00042 |
| $^{214}$Bi | 1543.3 | 0.00083 | 0.00045 | 0.00049 |
| $^{228}$Ac | 1580.5 | 0.00113 | | 0.00055 |
| $^{214}$Bi | 1583.2 | 0.00176 | 0.00044 | 0.00078 |
| $^{228}$Ac | 1588.2 | 0.00605 | 0.00187 | 0.00249 |
| $^{208}$Tl (DEP) | 1592.5 | 0.00619 | 0.00196 | 0.00274 |
| **$^{140}$La** | **1596** | | 0.00034 | |

| | | | | |
|---|---|---|---|---|
| $^{214}$Bi | 1599.3 | 0.00070 | | 0.00045 |
| $^{212}$Bi | 1620.5 | 0.00269 | 0.00109 | 0.00113 |
| $^{228}$Ac | 1625.1 | 0.00049 | | |
| $^{228}$Ac | 1630.6 | 0.00303 | 0.00137 | 0.00103 |
| $^{228}$Ac | 1638.3 | 0.00073 | | 0.00040 |
| $^{214}$Bi | 1661.3 | 0.00244 | 0.00087 | 0.00097 |
| $^{214}$Bi | 1684 | 0.00045 | | |
| $^{214}$Bi | 1729.6 | 0.00836 | 0.00388 | 0.00337 |
| $^{214}$Bi | 1764.5 | 0.03941 | 0.01624 | 0.01574 |
| $^{214}$Bi | 1838.4 | 0.00068 | | 0.00030 |
| $^{214}$Bi | 1847.4 | 0.00521 | 0.00218 | 0.00225 |
| $^{214}$Bi | 1873.1 | | | 0.00013 |
| $^{228}$Ac | 1887.1 | | | 0.00004 |
| $^{214}$Bi | 1890.3 | | | 0.00004 |
| $^{214}$Bi | 1895.9 | | 0.00010 | |
| $^{228}$Ac | 1955.9 | | | 0.00014 |
| $^{214}$Bi | 2016.7 | 0.00013 | | |
| $^{214}$Bi | 2052.9 | | 0.00013 | |
| $^{208}$Tl (SEP) | 2103.5 | 0.00587 | 0.00261 | 0.00214 |
| $^{214}$Bi | 2118.6 | 0.00235 | 0.00090 | 0.00100 |
| $^{214}$Bi | 2204.2 | 0.01056 | 0.00437 | 0.00442 |
| $^{214}$Bi | 2292.4 | 0.00071 | 0.00014 | 0.00018 |
| $^{214}$Bi | 2447.9 | 0.00310 | 0.00156 | 0.00102 |
| $^{208}$Tl | 2614.5 | 0.04015 | 0.01643 | 0.01647 |

Gamma-ray spectrum:

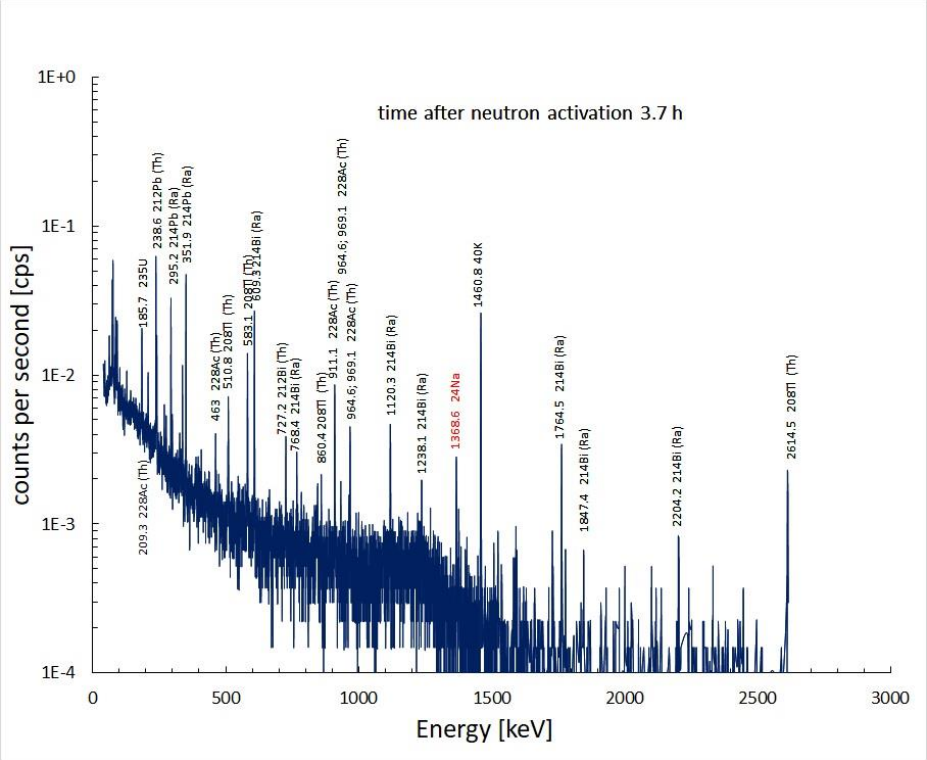


Fig. 58 Gamma-ray spectrum of a rock sample (sample 11) 3.7 h after neutron activation.

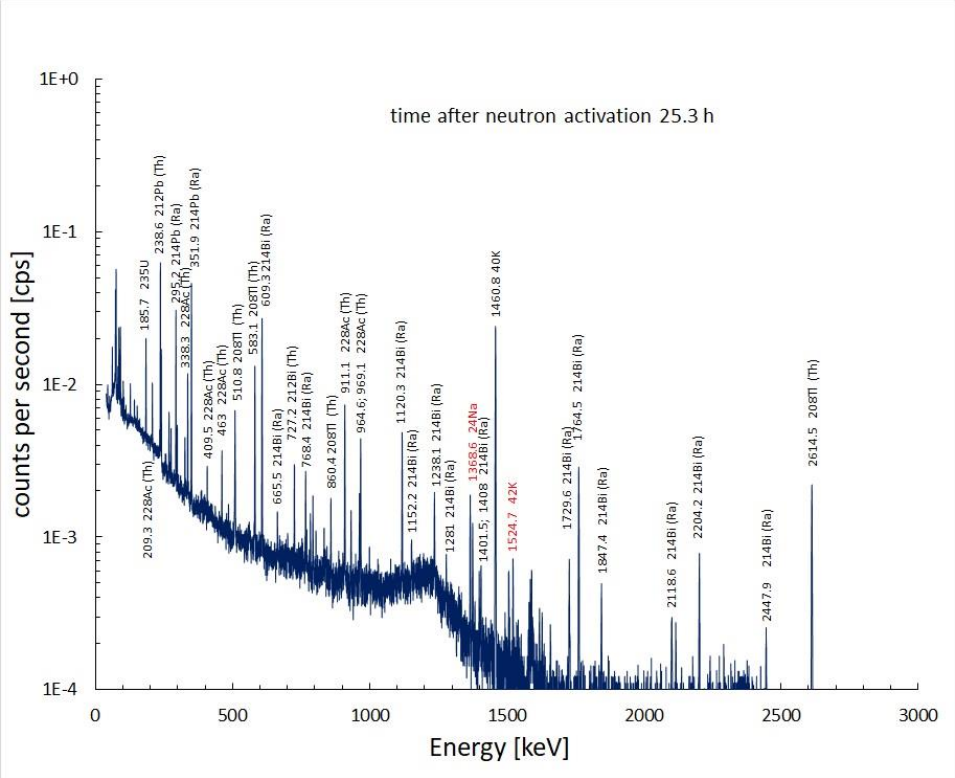


Fig. 59 Gamma-ray spectrum of a rock sample (sample 11) 25.3 h after neutron activation.

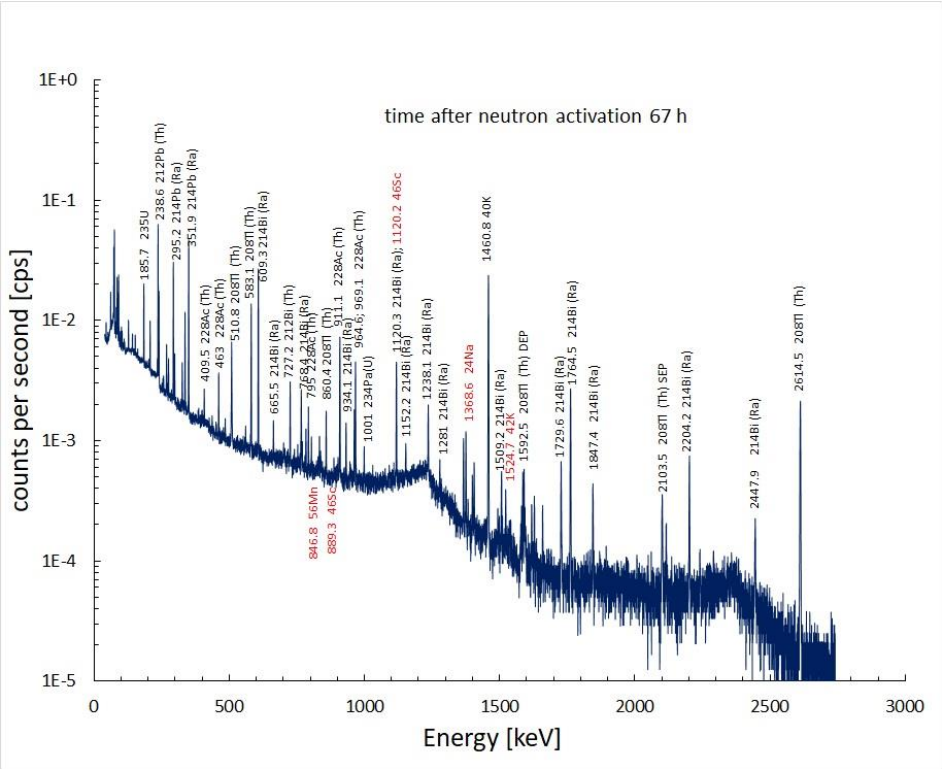


Fig. 60 Gamma-ray spectrum of a rock sample (sample 11) 67 h after neutron activation.

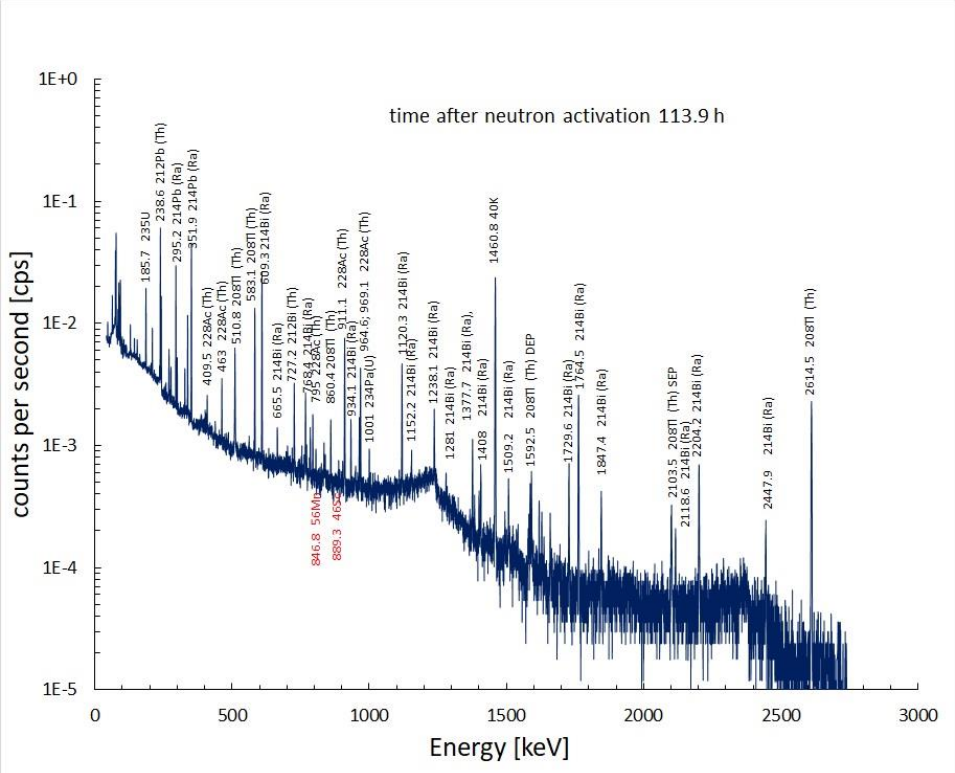


Fig. 61 Gamma-ray spectrum of a rock sample (sample 11) 113.9 h after neutron activation.

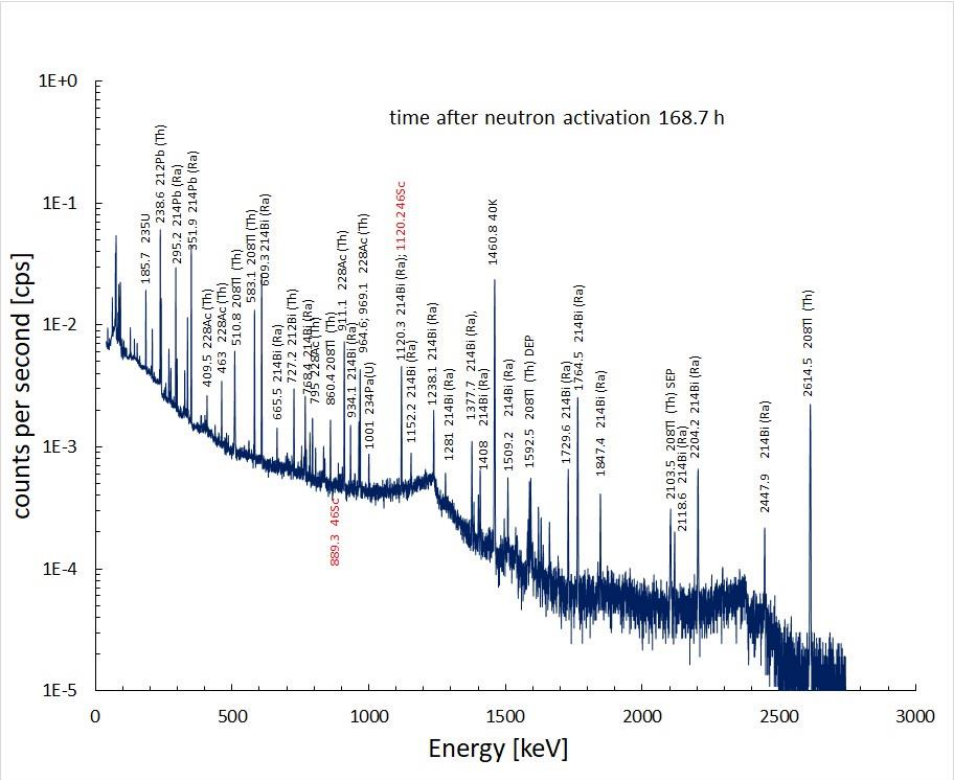


Fig. 62 Gamma-ray spectrum of a rock sample (sample 11) 168.7 h after neutron activation.

## *5.* Laboratory analyses of the sediment samples

Measurements of the concentration of radium and potassium radioisotopes in the sediment samples were performed in an external laboratory - "Low-level Activity Research Laboratory", Institute of Physics, the University of Silesia in Katowice, Poland.

Description of the sites where sediment samples were taken:

Tab. 15 Description of the sites where sediment samples were collected.

| **Hall ID** | **Depth below surface** [m w.e.] | **Sites** | **Method of the sampling** | **Name of the sample** |
|---|---|---|---|---|
| Localization 1 | 80 (layer 310) | floor | direct collection into plastic containers | Sediment sample loc.1 |
| Localization 2 | | | | Sediment sample loc.2 |
| Localization 3 | | | | Sediment sample loc.3 |
| Localization 4 | | | | Sediment sample loc.4 |
| Localization 5 | | | | Sediment sample loc.5 |
| Localization 8 | | | | Sediment sample loc.8 |
| Localization 9 | | | | Sediment sample loc.9 |

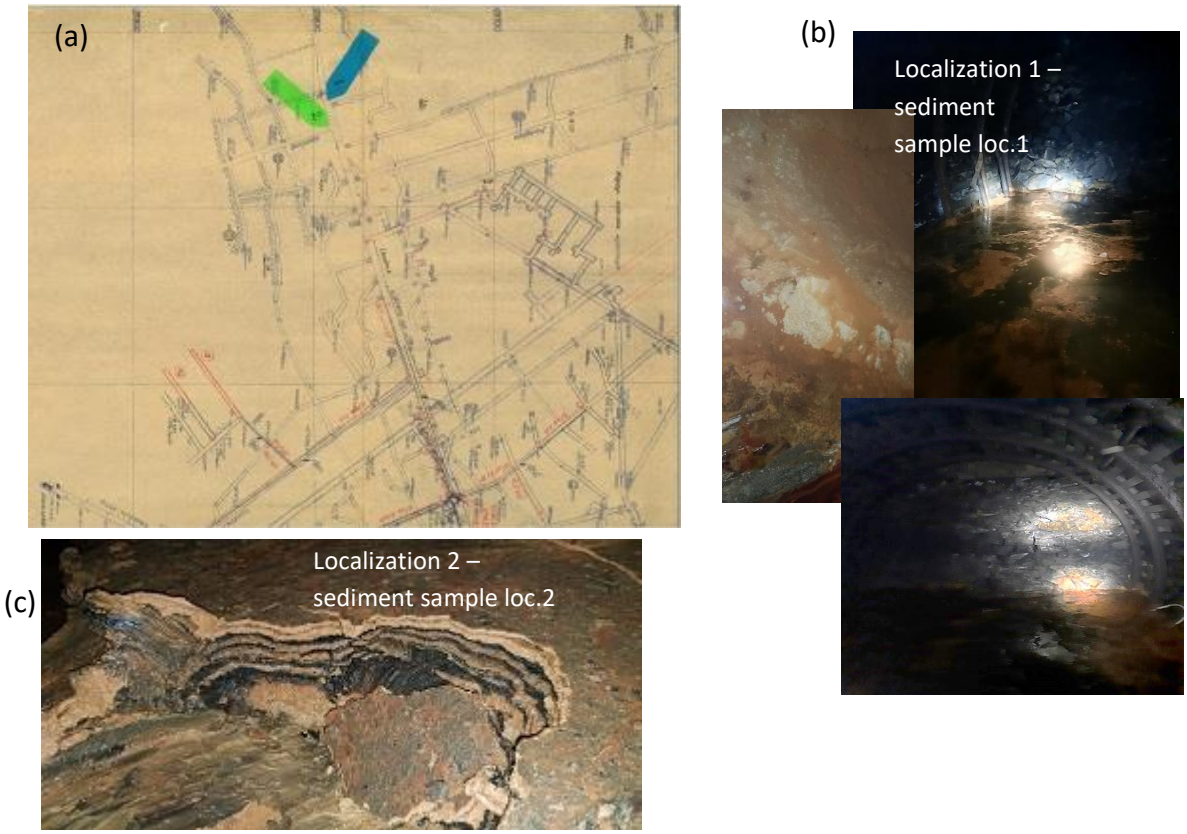


**Fig. 63 (a) diagram of the place where the samples were taken (b) localization 1 - sediment sampling, (c) localization 2 - sediment sampling.**

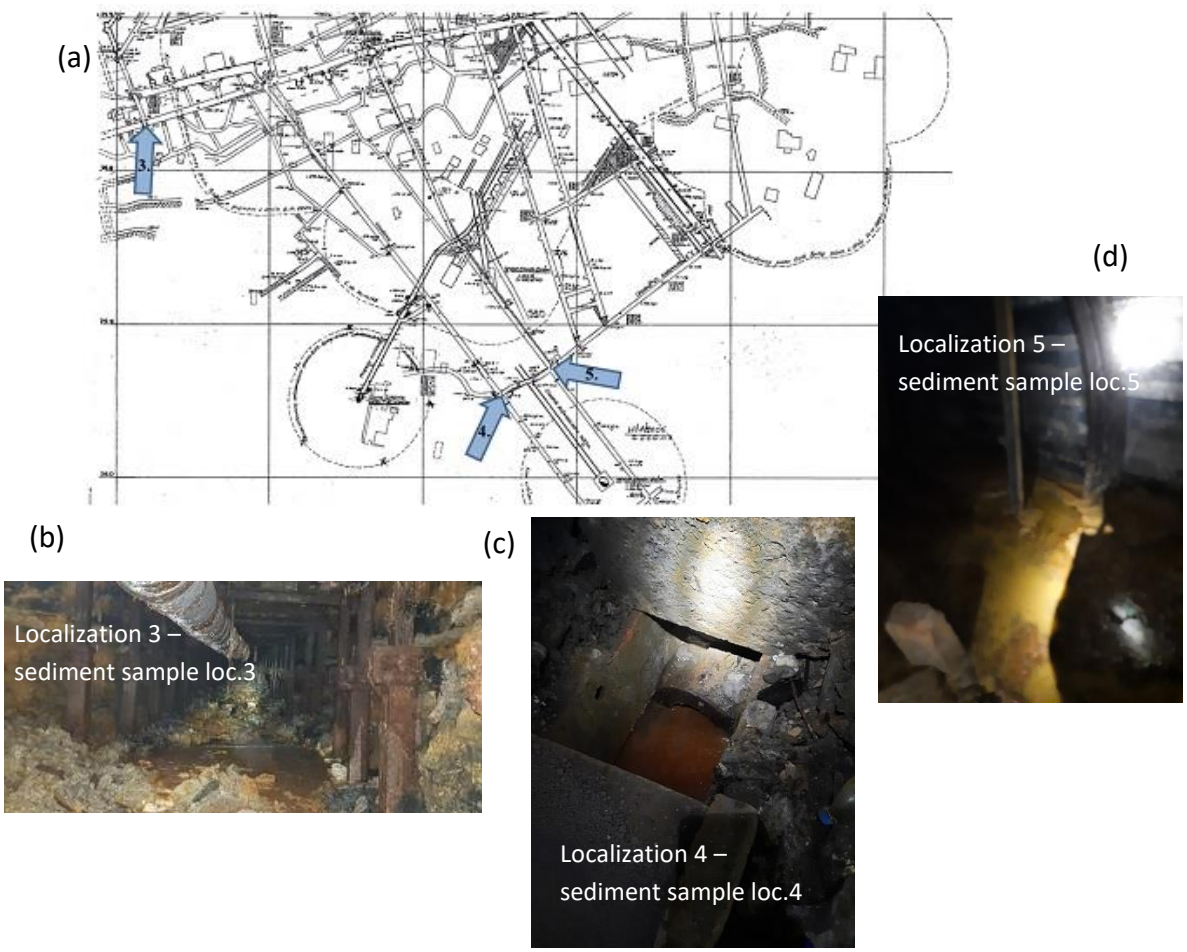


**Fig. 64 (a) diagram of the place where the samples were taken (b) localization 3 - sediment sampling, (c) localization 4 - sediment sampling, (d) localization 5 - sediment sampling.**

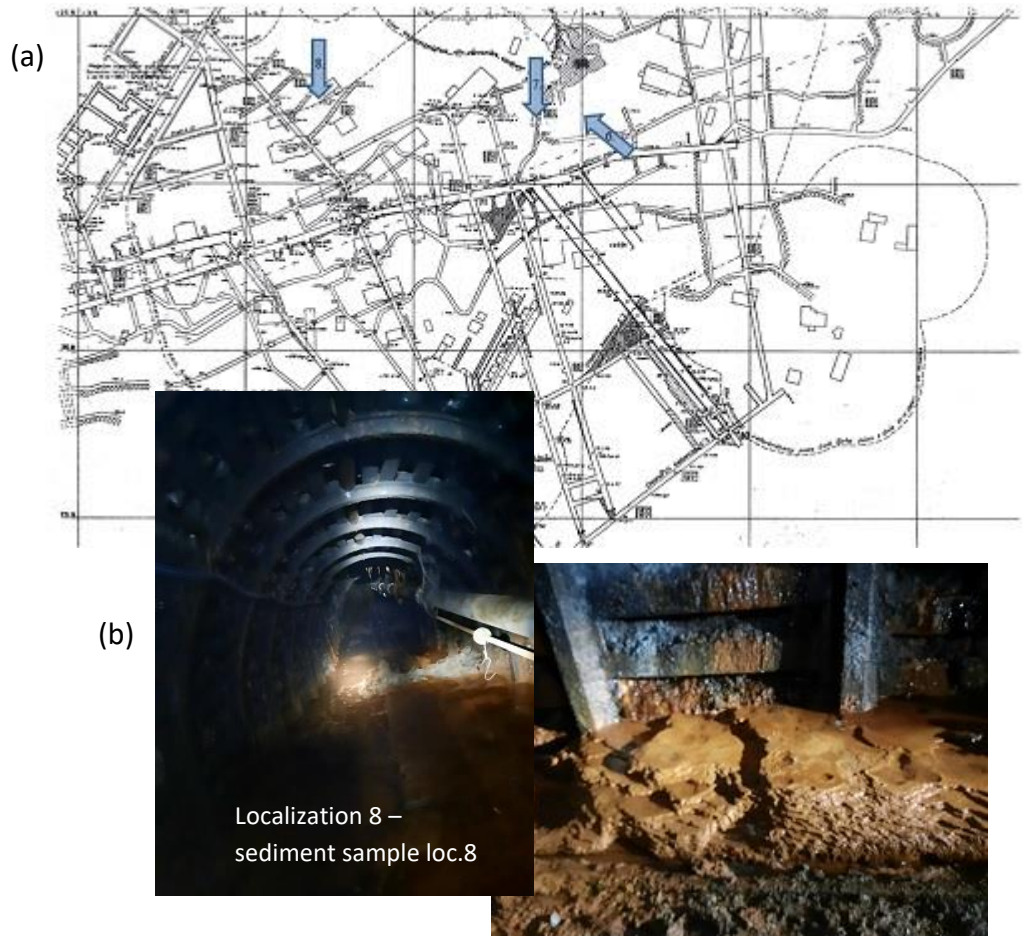


Fig. 65 (a) diagram of the place where the samples were taken (b) localization 8 - sediment sampling.

### *a. Radium and potassium concentration in sediment samples*

- Information about measurement

The concentration of radium and potassium isotopes in the sediment samples was determined by gamma spectroscopy with the HPGe detector in a lead shield (***Fig. 66a***). The activity of $^{40}$K was calculated directly from a single 1460.8 keV line. The activity of $^{226}$Ra was calculated as the weighted mean of the values obtained from the $^{214}$Pb (295.2, 351.9 keV) and $^{214}$Bi (609.3, 1120.3 keV) isotopes, while $^{228}$Ra activity was calculated from the gamma lines 338.3 keV and 911.1 keV originating from $^{228}$Ac decay. The total duration of a single measurement depended on the sample activity.

Description of the procedure performed before measurements and conditions during measurements (e.g. use of a Marinelli beaker; shielding of the detector; drying, crushing, grinding, mixing of rock; other relevant information): **Before the measurements, the sediment sample was**

**dried, crushed, ground, mixed and placed in a plastic container or in Marinelli beaker (Fig. 66b,c,d), which was then sealed and left for one month to achieve secular equilibrium in the thorium and uranium series. The grains diameter after crushing the sediment sample were less than 1 mm. Measurements were made in a shielded cover made of lead and copper.**

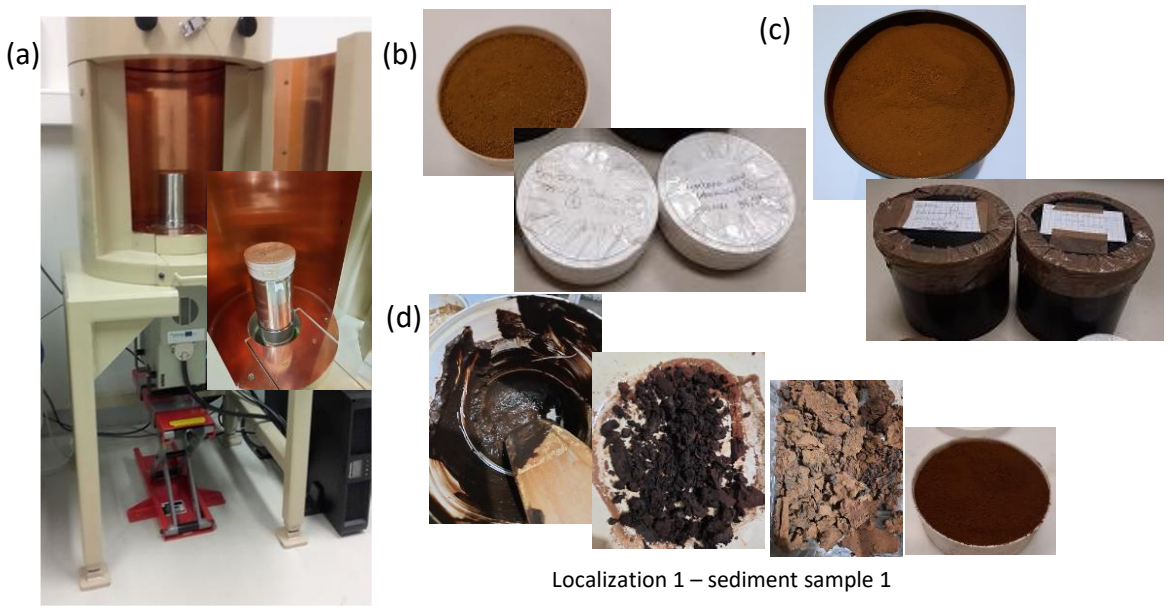


Fig. 66 (a) HPGe detector with shielding, (b) sediment sample in plastic container and (c) Marinelli beaker, (d) sediment sample preparation steps (drying).

Tab. 16 Results of radium and potassium concentration in sediment samples.

| Hall ID (name of sample) | Measu-rement method | Equipment type | Detection relative efficiency [%] | Collection period | Average results [Bq/kg] | | |
|---|---|---|---|---|---|---|---|
| | | | | | $^{226}$Ra | $^{228}$Ra | $^{40}$K |
| Sediment sample loc. 1 | Gamma spectro-metry | HPGe detector | 20 | 4.1 days | 92.9±3.4 | 270.5±4.8 | 41.3±1.5 |
| Sediment sample loc. 2 | | | | 2.9 days | 116.3±4.3 | 403.5±7.4 | 56.5±3.5 |
| Sediment sample loc. 3 | | | | 4.1 days | 32.3±0.3 | 257±11 | 211±13 |
| Sediment sample loc. 4 | | | | 2.0 days | 38.9±1.4 | 30.1±0.6 | 234.1±3.8 |
| Sediment sample loc. 5 | | | | 4.1 days | 20.3±0.7 | 30.1±0.6 | 223.8±3.5 |
| Sediment sample loc. 8 | | | | 2.2 days | 209.5±7.6 | 262.0±4.9 | 65.6±3.9 |
| Sediment sample loc. 9 | | | | 2.1 days | 58.1±2.1 | 39.8±0.9 | 486.1±8.7 |

Gamma-ray spectra:

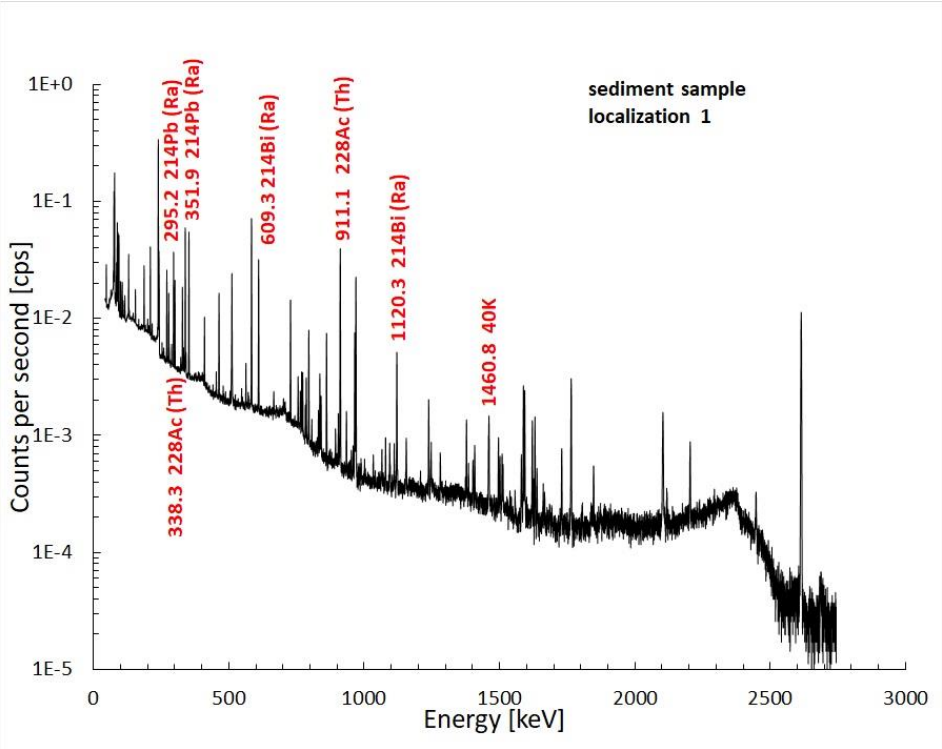


Fig. 67 Gamma-ray spectrum of a sediment sample loc.1.

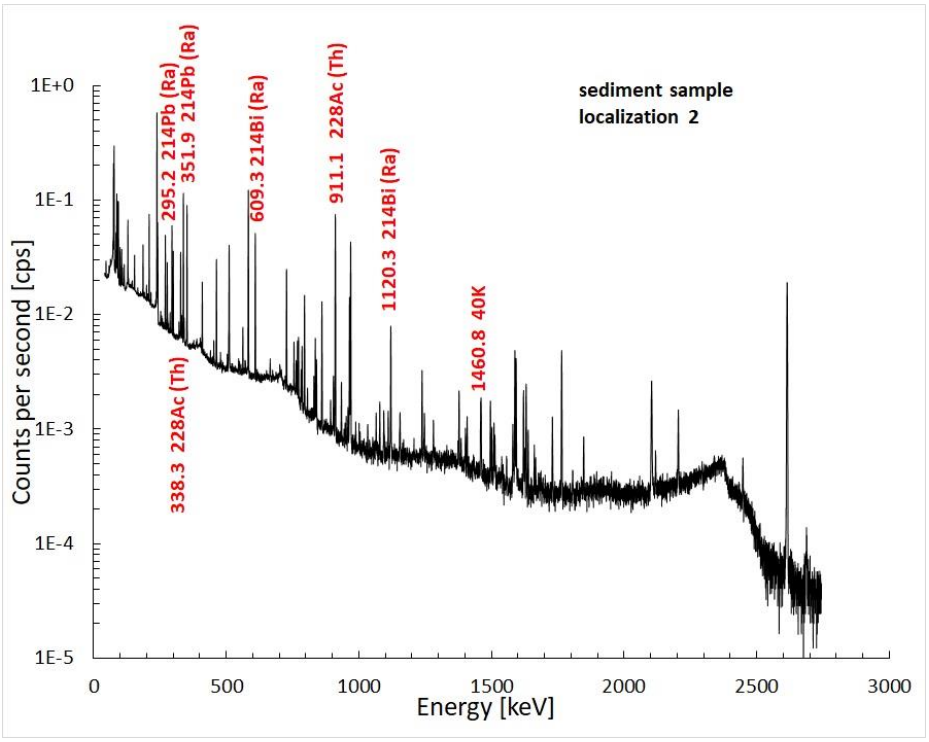


Fig. 68 Gamma-ray spectrum of a sediment sample loc.2.

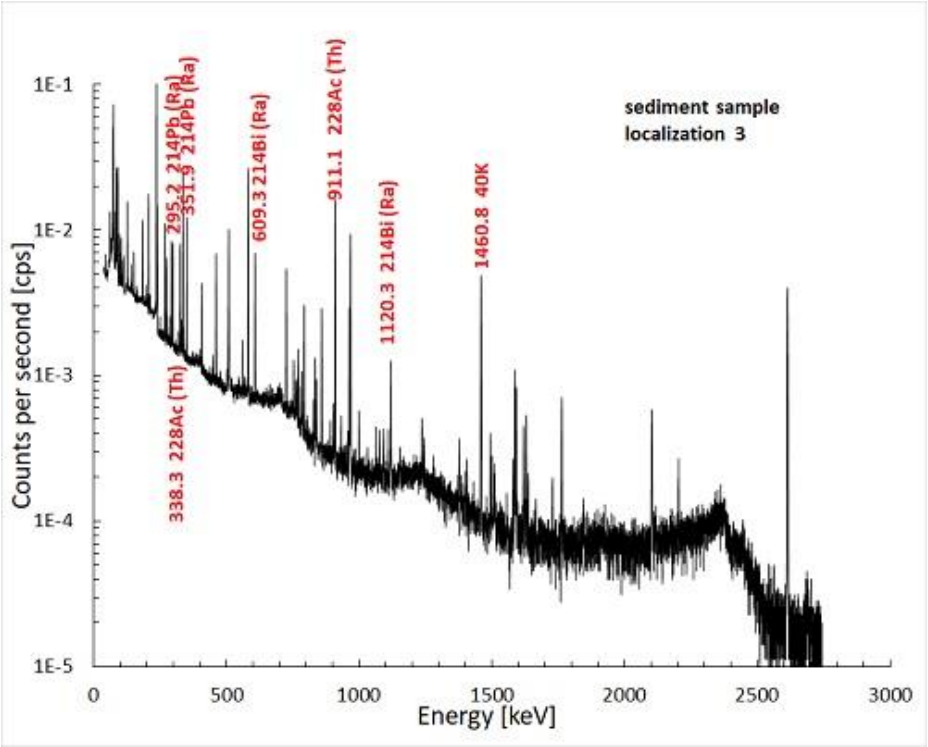


Fig. 69 Gamma-ray spectrum of a sediment sample loc.3.

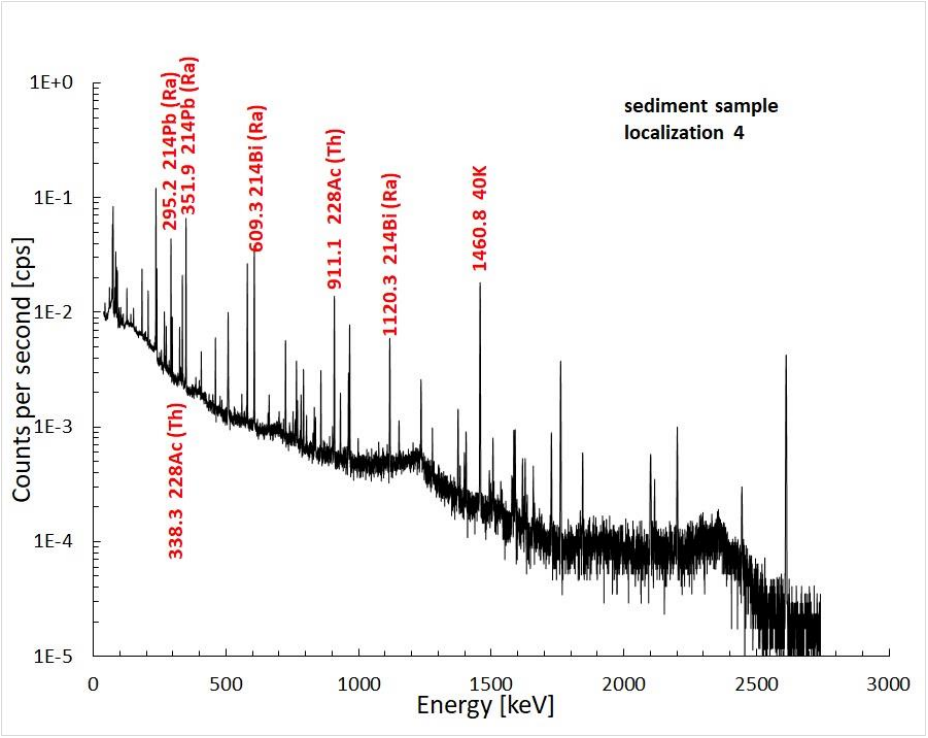


Fig. 70 Gamma-ray spectrum of a sediment sample loc.4.

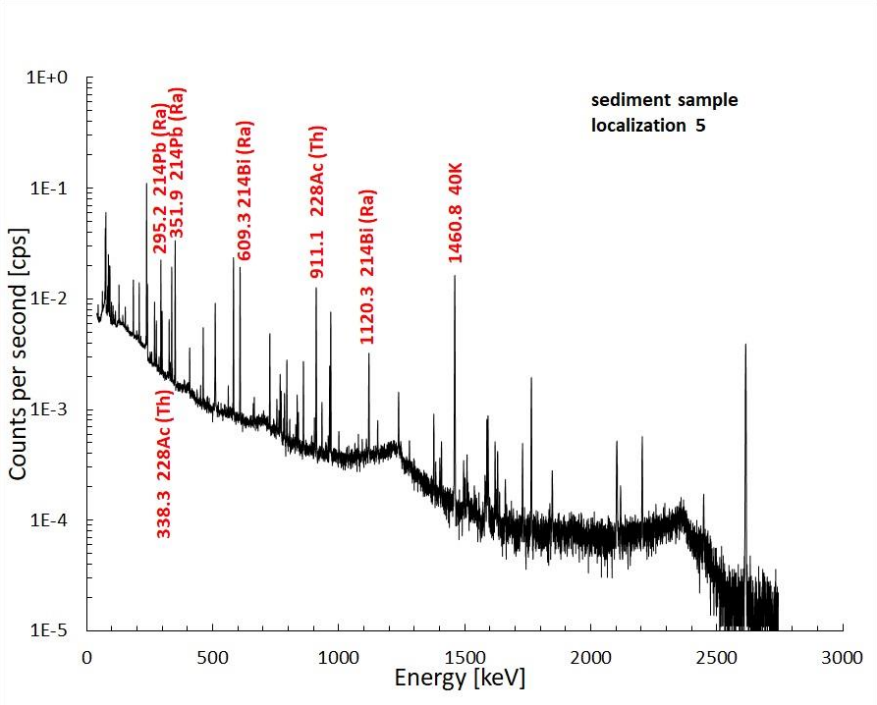


Fig. 71 Gamma-ray spectrum of a sediment sample loc.5.

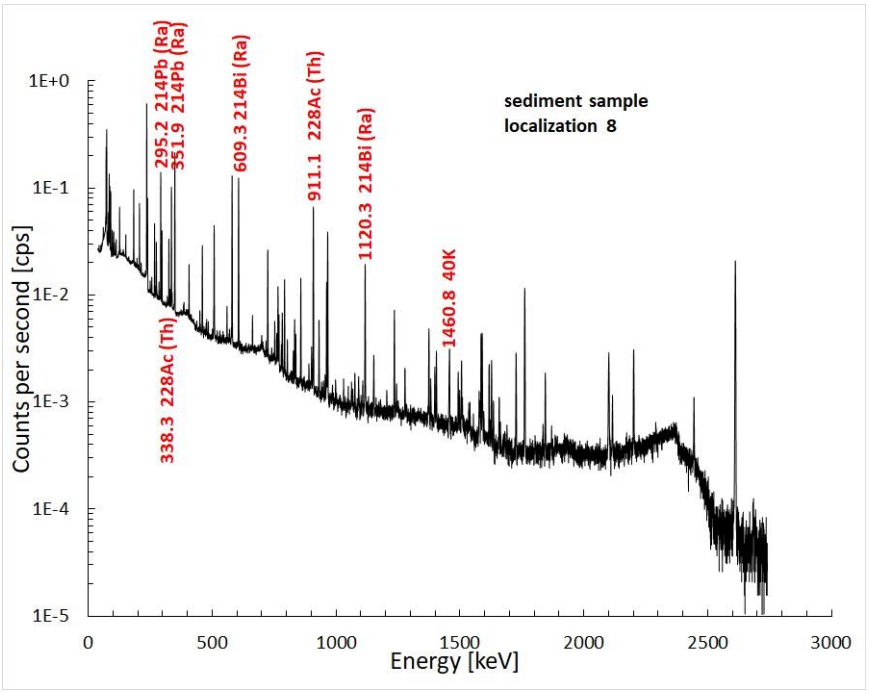


Fig. 72 Gamma-ray spectrum of a sediment sample loc.8.

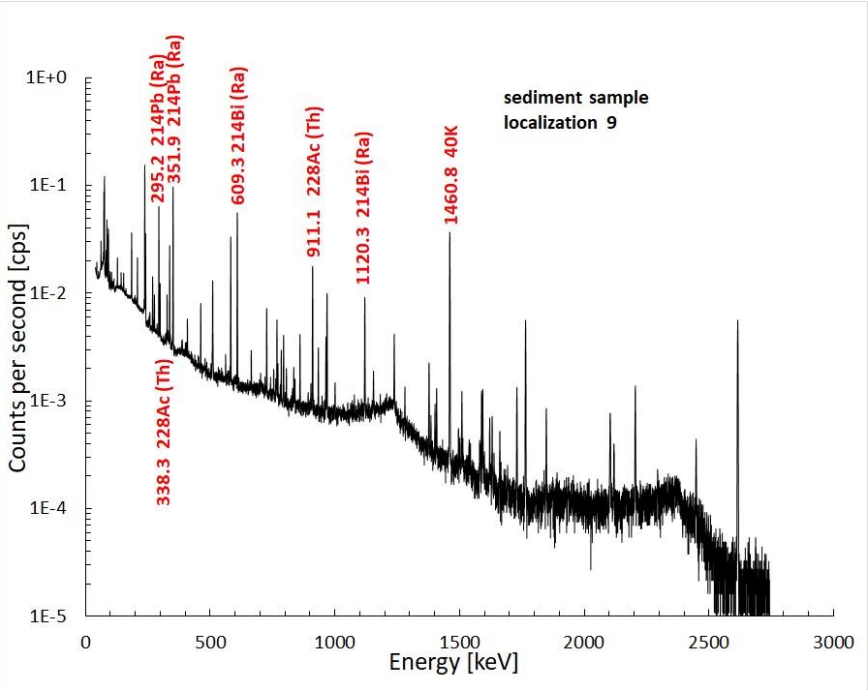


Fig. 73 Gamma-ray spectrum of a sediment sample loc.9.